Geoderma Regional 22 (2020) e00290

Contents lists available at ScienceDirect

Geoderma Regional

journal homepage: www.elsevier.com/locate/geodrs

Greenhouse gas emission from the cold soils of Eurasia in natural settings and under human impact: Controls on spatial variability

Dmitry Karelin [a,*], Sergey Goryachkin [a], Elya Zazovskaya [a], Vasily Shishkov [a], Alex Pochikalov [a], Andrey Dolgikh [a], Andrey Sirin [b], Gennady Suvorov [b], Nimazhap Badmaev [e], Natalia Badmaeva [e], Yuri Tsybenov [e], Anatoly Kulikov [e], Piotr Danilov [f], Grigory Savinov [f], Aleksey Desyatkin [g], Roman Desyatkin [g], Gleb Kraev [c,d]

[a] Institute of Geography RAS, Staromonetny 29, 119017 Moscow, Russia
[b] Institute of Forest Science, RAS, Uspenskoe, Sovetskaya 21, 143030 Moscow Region, Russia
[c] Institute of Physicochemical and Biological Problems of Soil Science, RAS, Puschino, Moscow Region, Russia
[d] Vrije Universiteit Amsterdam, Boelelaan 1085, Amsterdam, the Netherlands
[e] Institute of General and Experimental Biology, Siberian Branch of Russian Academy of Sciences, Ulan-Ude, Russia
[f] North-Eastern Federal University, Yakutsk, Russia
[g] Institute of Biological Problems of Cryosphere, Siberian Branch of Russian Academy of Sciences, Yakutsk, Russia

ARTICLE INFO

Article history:
Received 25 July 2019
Received in revised form 29 April 2020
Accepted 30 April 2020

Keywords:
Greenhouse gas
Emission
Land use
CO_2
Soil respiration
Nitrous oxide
Methane
Permafrost
Cryogenic soil
Tundra
Ultra-continental Siberia
Arctic
Cryosols
Cambisols

ABSTRACT

The annual balance of biogenic greenhouse gases (GHGs; carbon dioxide (CO_2), methane (CH_4), and nitrous oxide (N_2O)) in the atmosphere is well studied. However, the contributions of specific natural land sources and sinks remain unclear, and the effect of different human land use activities is understudied. A simple way to do this is to evaluate GHG soil emissions. For CO_2, it usually comprises 60–75% of gross respiration in natural terrestrial ecosystems, while local human impact can increase this share to almost 100%. Permafrost-affected soils occupying 15% of the land surface mostly in the Eurasia and North America contain approximately 25% of the total terrestrial carbon. The biogenic GHG soil emissions from permafrost are 5% of the global total, which makes these soils extremely important in the warming world. Measurements of CO_2, methane, and nitrous oxide, from eighteen locations in the Arctic and Siberian permafrost, across tundra, steppe, and north taiga domains of Russia and Svalbard, were conducted from August to September during 2014–2017 in 37 biotopes representing natural conditions and different types of human impact. We demonstrate that land use caused significant alteration in soil emission and net fluxes of GHGs compared to natural rates, regardless of the type and duration of human impact and the ecosystem type. The cumulative effect of land use factors very likely supported an additional net-source of CO_2 into the atmosphere because of residual microbial respiration in soil after the destruction of vegetation and primary production under anthropogenic influence. Local drainage effects were more significant for methane emission. In general, land use factors enforced soil emission and net-sources of CO_2 and N_2O and weakened methane sources. Despite the extended heat supply, high aridity caused significantly lower emissions of methane and nitrous oxide in ultra-continental Siberian permafrost soils. However, these climatic features support higher soil CO_2 emission rates, in spite of dryness, owing to the larger phytomass storage, presence of tree canopies, thicker active layer, and greater expressed soil fissuring. Furthermore, the “Birch effect” was much less expressed in ultra-continental permafrost soils than in permafrost-free European soils. Models and field observations demonstrated that the areal human footprint on soil CO_2 fluxes could be comparable to the effect of climate change within a similar timeframe. Settlements and industrial areas in the tundra function as year-round net CO_2 sources, mostly owing to the lack of vegetation cover. As a result, they could compensate for the natural C-balance on significantly larger areas of surrounding tundra.

1. Introduction

There are three main biogenic greenhouse gases (GHGs) in the focus of global ecology: carbon dioxide (CO_2), methane (CH_4), and nitrous oxide (N_2O). Among them, CO_2 is the most important actor in contemporary organic matter turnover on the Earth. If our ultimate goal in this particular field of study were to estimate the dynamics and environmental controls of terrestrial organic matter cycling, would we measure the CO_2 efflux or emission from soil (soil respiration (SR)) instead of the net flux (NF)? In other words, why should one estimate a single component instead of the whole thing? There are several reasons:

* Corresponding author.
E-mail address: dkarelin7@gmail.com (D. Karelin).

https://doi.org/10.1016/j.geodrs.2020.e00290
2352-0094/

(i) Soil is holistic and the most important component of any terrestrial ecosystem with its specific C-balance controls;
(ii) CO_2 efflux from soil is the largest component of gross respiration for land ecosystems (almost 80% in land and 50% globally) actively involved in climate change positive feedbacks (Tarnocai et al., 2009). Additionally, 47% of CH_4 and 53% of N_2O global annual emissions relate to soil degassing (Solomon et al., 2007; Oertel et al., 2016);
(iii) SR is used to monitor and compare the functional state of different terrestrial ecosystems (the fastest response to environmental change). It is a good indicator in disturbed ecosystems. For example, the assessment of response to changing climate requires long-term studies of SR in the key ecosystems. However, study of the effect of land use on natural ecosystems requires comparison of short-term SR measurements at representative disturbance sites;
(iv) SR is necessary to specify in compartment and simulation modeling of C-balance of ecosystems at different scales and to verify net C-balance models. Not surprisingly, the best C-cycle models, such as DNDC or RothC, finely represent soil processes and biogenic GHG balance between soil and the atmosphere (International Soil Modeling Consortium, https://soil-modeling.org/resources-links/model-portal). Additionally, wide variability in the ratio between root and microbial respiration in soils (Kuzyakov, 2006) forces one to measure a combined CO_2 efflux;
(v) Finally, it is simple to measure soil surface emission of CO_2 or exchange of other GHGs, as compared to their net fluxes.

SR measurement remains the simplest and the most effective method of complex ecosystem assessment. The number of articles containing keywords “CO_2 soil emission” exceeds that of articles with “CO_2 net flux” (5541 > 4075) among studies published over the last 10 years according to ScienceDirect search engine.

Currently, humankind can precisely estimate the global carbon sink using the difference between the annual volumetric increment of CO_2 in the atmosphere and the global annual anthropogenic C emissions, which we believe are being evaluated correctly. However, human C emissions cannot be attributed to fossil fuel combustion only, and the C-sinks are not exclusively natural. We still do not fully account for the shift in C-exchange due to human land use at the local scale, which could significantly add to both the first and second term of the calculation. This is also true for the cycles of other biogenic GHGs driven by the C-cycle.

Normally the terrestrial ecosystem is in balance between incoming and outgoing carbon (C–CO_2) fluxes, because incoming production and outgoing respiration fluxes seek an equilibrium position. After a land use event, or any terrestrial human disturbance, usually the above ground primary production is eliminated, which in the next time step will result in a decrease of below ground production and respiration flux down to its non-rhyzospheric microbial component. However, this happens with a delay (sometimes it takes years) and hence, there is a period during which the ecosystem becomes a carbon source to the atmosphere until (or if) a new equilibrium is reached. Microbial GHG emission exists until organic matter is available. Soil respiration is the sum of root and microbial respiration including the rhizosphere. Normally in forests, it comprises approximately 70% of gross respiration, while in tundra and cryogenic boreal communities it is 90% or higher due to small above-ground vegetation component, as compared to its below-ground pool, and to the large soil organic pool. By our estimates, in human-affected cryogenic ecosystems the input of this component can reach 95–99% of gross respiration.

The permafrost zone in Eurasia, occupying approximately half of the global permafrost area, is among the most vulnerable biomes with one of the greatest immobilised C-pools in perennial and seasonally frozen grounds (Karelin and Zamolodchikov, 2008). Most of this vast frozen body is located in Russia (French, 1996). Nevertheless, few studies are devoted to estimation of GHG fluxes in human-affected territories in cryogenic areas of Eurasia (Petrescu et al., 2015; Stark et al., 2015).

Over the recent 40 years, the tundra biome acted as a carbon sink during the growing season. Summer phytomass production exceeded the decomposition of organic matter because of the global rise in atmospheric CO_2 and the climate warming. However, on an annual scale, tundra remained the source of atmospheric carbon (see review by Belshe et al., 2013). There is little understanding of the quantitative assessment of the effect of land use, which can convert atmospheric carbon sinks to sources acting either in concert with climate change or alone (Schulze et al., 2009; Karelin et al., 2017b).

Features of soil emissions of CO_2 and other biogenic GHGs related to extreme conditions of continental cryoarid regions of central and eastern Eurasia in Russian territory are also of interest as these regions are unique for the biosphere. The soils of these areas were subject to a specific extra-continental climate with a cold winter and a dry short summer (Williams and Smith, 1989) over the Holocene, owing to the large distance to oceans. Other exceptional features include a low annual temperature in the region, the home to the Pole of Cold of the ice-free lands and occurrence of 300–1000 m-thick cold permafrost in Central Yakutia (French, 1996). However, larch-birch forests prevail among the ecosystems of this region. They adapt to the extreme conditions because of sufficient summer air temperatures for these woody species over the growth season. In addition to the annual temperature and precipitation regime, we need to test the contribution of freezing-related nano-, micro-, and meso-relief to CO_2 emission from soils. This factor acts in tundra by controlling the water table, soil moisture, nutrient storage, wintering conditions for the plants, community species composition, above-ground phytomass, and preservation of permafrost, the “glue” for this ecosystem (Karelin and Zamolodchikov, 2008). This is why destruction of the protective vegetation cover by human (grazing, agriculture, and construction) or natural (fires, windthrows, and phytophags) actors causes intensive permafrost degradation, badland formation (Desyatkin et al., 2007), or long-term alteration of the ecosystem structure (Zamolodchikov et al., 1998a, 1998b; Karelin and Zamolodchikov, 2008). Features of continental communities of the Eurasian permafrost zone are understudied as compared to tundra.

Carbon footprinting of arctic settlements is another important and poorly studied subject (Pandey et al., 2011). The challenge is to understand how the condensed zones of human impact, which transform the Arctic landscapes, affect the carbon exchange of their surroundings and what are the contributions of the components of the exchange, including SR. The effect of local land use controls might be comparable or stronger than those of climate change over a period of time (Karelin et al., 2016, 2017b). However, global climate change caused by human activities, including the warming and alteration of precipitation, acts similarly both on intact and modified cryogenic ecosystems. The differences in the response, however, remain unclear. In this study, we explore how various types of human land use of the permafrost territories in Eurasia affect GHG fluxes, with a special emphasis on carbon dioxide. Another important issue is the assessment of their spatial contribution and the specific drivers of GHG emissions within continental permafrost limits.

2. Materials and methods

2.1. Regional settings

Over 4 years (2014–2017) we monitored six cryogenic sites in the Eurasian Arctic zone from arctic, typical and shrub tundra to north boreal forests, and from North Europe to the Russian Far East. Each site represents several monitoring plots with different types of human land use. Field data were collected during the vegetative seasons in July–August (with exceptions for “Vorkuta” and “Lorino” sites, which were also processed in September), when the soil and net fluxes of

GHG were maximal. We consider the arctic, subarctic, non-permafrost north-boreal, and ultra-continental steppe or forest permafrost ecosystems as cryogenic, due to the similar low temperature limitations of organic matter exchange. Nevertheless, most of the sites were located in continuous permafrost zones (Table 1, Fig. 1). The detailed descriptions of these sites are available (Karelin et al., 2016 (sites 1–6); Karelin and Zamolodchikov, 2008 (sites 1, 4)).

In addition, twelve selected mobile (measured only once) sites in the ultra-continental permafrost inland areas of Russia were studied by the research team in August 2017 along the trans-Siberian route from Ulan-Ude (Buryat Republic of Russian Federation) to Chita (Chita region), then to Yakutsk and Oymyakon (Sakha Republic of Russian Federation) (Fig. 1, Table 1, sites 7–18), covering 3840 km in total distance. These sites included micro-sites (37 overall) distinguished by different micro-relief due to extreme cryoturbation or desiccation processes, with different vegetation types, slopes, or orientations. High soil and local climatic condition diversity are found on the southern permafrost boundary in Buryat Republic. Driven by climate change, permafrost has degraded and its boundary retreated over the last century, with the fastest rate observed in open landscapes and the lowest in forests (Badmaev and Bazarov, 2018). The most pronounced cryogenic features were found in the Republic of Sakha (Yakutia), with the thickest permafrost in the world found in the Central Yakutia (French, 1996). Detailed documentation of sites was published in the following sources: sites 7 and 11 (Badmaev and Bazarov, 2018), site 10 (Kovda et al., 2017), sites 8–11 (Badmaev et al., 2009), and sites 13 and 14 (Desyatkin et al., 2007). Such large-scale SR measurements were made in the region for the first time in this study.

2.2. Land use effects in cryogenic areas

First, major human local land use effects on the C-balance in cryogenic ecosystems were identified and classified (a–f, see below), based mostly on our long-term field data on CO_2 soil emissions.

(a) Permafrost degradation is a remarkable and widely discussed effect of land use on C-balance. In the majority of cases, permafrost thawing is due to direct continuous warming and increase in ground bulk density by buildings, industrial constructions, human trampling, and vehicles and heavy machinery, as well as the destruction and/or removal of natural soil/vegetation cover due to construction or farming. The territory of human settlements /industrial zones is subjected to strong constant trampling and load pressure from heavy machinery and vehicles. Warming and thawing of permafrost under such mechanical loads is at least partly mediated by an increase in bulk density of soils and sediments and the resulting loss of thermal insulation. Normally a progressive thawing of permafrost leads to increase in CO_2 soil emission and converts the affected territory into a net C-source to the atmosphere.

(b) Second is a separate impact of *human trampling, or load pressure* from heavy machinery on soil bulk density, or soil carbon dioxide storage in porous soil media and absorption by solid soil particles. Greater soil density may either increase or decrease in CO_2 soil emission, depending on the longevity of the impact. The instantaneous effect of physical pressure (load) leads to a transient but significant rise in soil CO_2 emission mostly due to desorption of CO_2 molecules from soil (Smagin et al., 2016), whereas long-term trampling reduces emissions due to elimination of vegetation. However, in all cases the "trampling effect" results in a shift from a net C sink to a source to the atmosphere. Examples include human trails, railways, ATV tracks, country roads, motorways of different age, and settled territories. In the northern taiga, these activities also include logging plots.

(c) Next, the effect of land use can have a direct *chemical influence* through landfills, garbage collectors, contamination by fuel leaks, industrial storage or warehouses, and special cases of animal husbandry, or butchering. This can result in either increases or decreases in soil CO_2 emission and increases/decreases in net C-source to atmosphere.

(d) *Fires* are another human effect on the ecosystems. The evolution of CO_2 emissions is driven by succession chronology. The C-source formed at first stage gradually shifts to C-sink during middle stages (Zamolodchikov et al., 1998a, 1998b). Depending on the succession stage in post-fire history CO_2 emission and net C source can be promoted in the early stages, or transform to a net C-sink in the middle stages (Zamolodchikov et al., 1998a, 1998b). This is because of the elimination of vegetation by fire followed by thawing, with subsequent dominance of soil respiration over gross primary production in the first years, and increase in carbon sink during active plant growth.

(e) The effect of *farming, ploughing, land cultivation, grazing, mowing,* and *forest clear-cut logging (in the northern taiga)*. Although this type of land use most strongly affects carbon balance worldwide, in cryogenic ecosystems this is rare in practice. Among studied ecosystems, the effect of farming or land cultivation is partly expressed only in the European northern taiga zone (mostly these are local vegetable garden plots, where permafrost is lacking), and the effect of grazing occurs in ultra-continental permafrost areas of Eurasia. The land cultivation and moderate pasturing normally result both in rise of gross primary production and gross respiration fluxes, with a dynamic neutral C-balance shifting between C-sink and source. The only difference from natural ecosystems is that net primary production in this case is consumed by humans. Long-term intensive arable farming and overgrazing commonly lead to decreases in soil C emission and increases in net C-source. A special case of this type of land use is domestic reindeer grazing sites in tundra, where over-pasturing commonly results in pasture digression and serious degradation of the soil cover and thus, in continuous net C-source to the atmosphere.

(f) Finally, another important land use effect in cryogenic ecosystems was discovered, which we call "the embankment effect", which can be considered a unique feature of tundra ecosystems. Shelter-like artificial relief elements, like depressions, embankments, earthen or gravel berms, subgrades and shoulders of gravel roads, motorways, railways, or airfields and buildings promote a rise in primary production and respiration fluxes, with higher winter emission and temporary (for several years) rise in net C-sink. All these artificially created positive and negative forms of micro- and meso-relief act as valuable warmer shelters for wintering tundra plants, accumulating snow-packs and inducing the increase of under-snow temperatures. This effect is exceptionally pronounced along the embankments or elevated subgrades of railroads in tundra, even though they widely occur in relief depressions because of the warming effect of the thicker snowpack (Karelin and Zamolodchikov, 2008). The overall effect of embankments on SR is positive (see Section 2.7 for explanation), because higher rates of SR, which include respiration of roots and microbiota, follow the increase in plant primary production. As a result, the ecosystem turns into a carbon sink or maintains carbon exchange balance.

It is necessary to note that many of the above-mentioned effects are acting in concert. Thus, warming, soil/vegetation removal or destruction, chemical contamination, trampling, and the embankment effect are all caused by coal mining or construction of gas/oil drilling rigs and pipelines.

Table 1
Brief description of the studied sites.

Site number (by Fig. 1) and name	Coordinates; elevation	Type of natural ecosystem	Type of permafrost (maximal seasonal thaw depth, m)	Years of study (number of soil CO_2 efflux measurements)	Type of natural soil (WRB)	Effects of human land use presented at the site[a]
1. Vorkuta region (Komi Republic, Russia)	N67°20′, E64°44′; 120 m a.s.l.	South shrub tundra, northern limit of forest tundra	Sporadic (0.5–1.7)	2014–2017 (1228)	Reductaquic Turbic Cryosol, Gleyic Cambisol, Histic Reductaquic Turbic Cryosol	(a–f)
2. Naryan-Mar (Nenets region, Russia)	N67°38′, E53°32′; 30 m a.s.l.	South shrub tundra, peat bogs	Discontinuous (0.5–2)	2014 (107)	Spodic Turbic Cryosol, Cryic Histosol, Reductaquic Turbic Cryosol, Gleyic Cambisol	(e)
3. Pinega (Arkhangelsk region, Russia	N64°42′, E43°23′; 30 m a.s.l.	Northern taiga (*Pinus sylvestris, Picea abies*)	Permafrost-free, seasonal freezing	2014–2017 (582)	Albic Podzol, Retic Podzol, Albic Luvisol	(a–e)
4. Lorino (Eastern Chukotka, Russia)	N65°30′, W171°43′; 12 m a.s.l.	Far East mossy tundra, settlement area	Continuous (0.55)	2013 (175)	Oxyaquic Turbic Cryosol	(a–e)
5. Barentsburg (Svalbard, Norway)	N78°05′, E14°12′; 40 m a.s.l.	Patchy arctic tundra	Continuous (0.80)	2014–2017 (360)	Turbic Cryosol (Fluvic, Humic)	(a–e)
6. Bovanenkovo (Yamal Peninsula, Russia)	N70°23′, E68°29′; 23 m a.s.l.	West Siberian mossy tundra, pipeline zone	Continuous (0.5–1.7)	2015 (45)	Reductaquic Turbic Cryosol	(a, b)
7. B1 (Khorinsk, Republic of Buryatia)	N52°19.5′, E110°13′; 735 m a.s.l.	Steppe, medium grazing load	Sporadic (2.4–2.45)	2017 (15)	Haplic Calcisol Arenic	(e)
8. B2–1 (Komsomolskaya sopka, Republic of Buryatia)	N52°28′ E111°04′; 898 m a.s.l.	Forest steppe, open larch-birch forest, 2–3° North slope, traces of fire and cuttings	Discontinuous (2–3)	2017 (30)	Stagnic Phaeozem (Tonguic)	(d, e)
9. B2–2 (Komsomolskaya sopka, Republic of Buryatia)	N52°28′, E111°04′; 880 m a.s.l.	Forest steppe, 8–9° South slope,10-yr-old fallow, moderate grazing load	Discontinuous (2–3)	2017 (15)	Eutric Cambisol (Protocalcic)	(e)
10. B3 (Krasnaya Gorka, Republic of Buryatia)	N52°39.1′, E111°24.7′; 978 m a.s.l.	Forest steppe, steep south slope	Discontinuous (2.80)	2017 (15)	Haplic Vertisol (Stagnic)	(e)
11. B4 (Eravna, Republic of Buryatia)	N52°30.5′, E111°32.4′; 933 m a.s.l.	Forest steppe, steppe meadow	Discontinuous (2.75–2.8)	2017 (15)	Luvic Chernozems (Stagnic, Tonguic)	(a, b)
12. S1 (Shilka, Chita region)	N51°58.5′, E115°55.2′; 628 m a.s.l.	Forest steppe, steppe meadow	Discontinuous to sporadic (2.8–3)	2017 (15)	Greyzemic Phaeozem (Tonguic, Turbic)	(e)
13. AL1 (Yakutsk, Sakha Republic)	N62°28.5′, E130°56.7′; 132 m a.s.l.	Alas depression and larch-birch forest	Continuous (3)	2017 (25)	Stagnic Cambisol (Humic)	(e)
14. PAL-1 (Yakutsk, Sakha Republic)	N62°28.4′, E130°59′; 135 m a.s.l.	Larch-birch forest	Continuous (1.17)	2017 (15)	Luvic Turbic Cryosol (Albic)	(d)
15. O1 (Oymyakon, Sakha Republic)	N63°15.7′, E143°10.6′; 849 m a.s.l.	Steppe-meadow, southeastern slope	Continuous (1.5)	2017 (15)	Leptic Kastanozem (Tonguic, Turbic)	(d)
16. O2 (Oymyakon, Sakha Republic)	N63°15.5′, E143°10.8′; 851 m a.s.l.	Larch-birch forest (70 yr), north slope	Continuous (1.2)	2017 (15)	Leptic Albic Podzol (Turbic)	(d)
17. KR1 (Sakha Republic)	N63°26.1′, E140°33.1′; 1096 m a.s.l.	Open larch-birch forest	Continuous (0.98)	2017 (15)	Turbic Cryosol (Thixotropic)	(d)
18. P1 (Sakha Republic)	N62°36′, E134°1.8′; 236 m a.s.l.	Larch-birch forest	Continuous (1–1.5)	2017 (15)	Luvic Turbic Cryosol	(d)

[a] Effects of land use are described in Section 2.2.

2.3. Measurements of soil emissions of GHGs

Points of measurements were classified by particular types of human impact within every site. In certain cases, like the coalmine complex at the Vorkuta site, the measurements were performed to characterise the effect of the full spectrum of types of human impacts. The control plots with background emissions were chosen in dominantly intact ecosystems close to disturbed habitats.

The flux measurement technique was similar at all stationary sites (sites 1–6, Table 1) and on the Siberian transect (sites 7–18). Soil CO_2 fluxes were measured in closed chambers with portable infrared analysers Li-6200, Li-6400, and Li-8100A (LiCor, Nebraska, USA), and field gas analysers constructed on the base of CO_2/temperature/humidity sensor AZ-7755 (https://www.az-instrument.com.tw/az-instrument/en/productsinfo/15.html, Taiwan, China). The AZ-7755 analysers were calibrated in the field by the high-precision analysers Li-6200, Li-6400, and Li-8100A, which in turn were calibrated using gas standards. We used chamber bases of 15–30 cm-long opaque polyvinyl chloride tubes, with basal area of 95 cm^2 and volume of 1–2 l. Open chambers were inserted into the soil at 3–4 cm depth, then after 2 h were tightly closed with a lid, connected by cellulose tubes to gas analyser for 3–6 min, depending on the flux rate. At each plot, SR measurements were taken at 10–20 points, located either linearly at a distance of 5–10 m from each other or in specific microhabitats. To better fit to daily values, soil efflux measurements in July–September were mostly made in the morning (between 8 and 10 a.m.) or evening (6–8 p.m.), when instantaneous emission of CO_2 from soils in Arctic ecosystems corresponds to mean diurnal rate (Karelin and Zamolodchikov, 2008). During installation of chamber bases, stems and shrub roots were avoided, and the live parts of other plants including the tops of

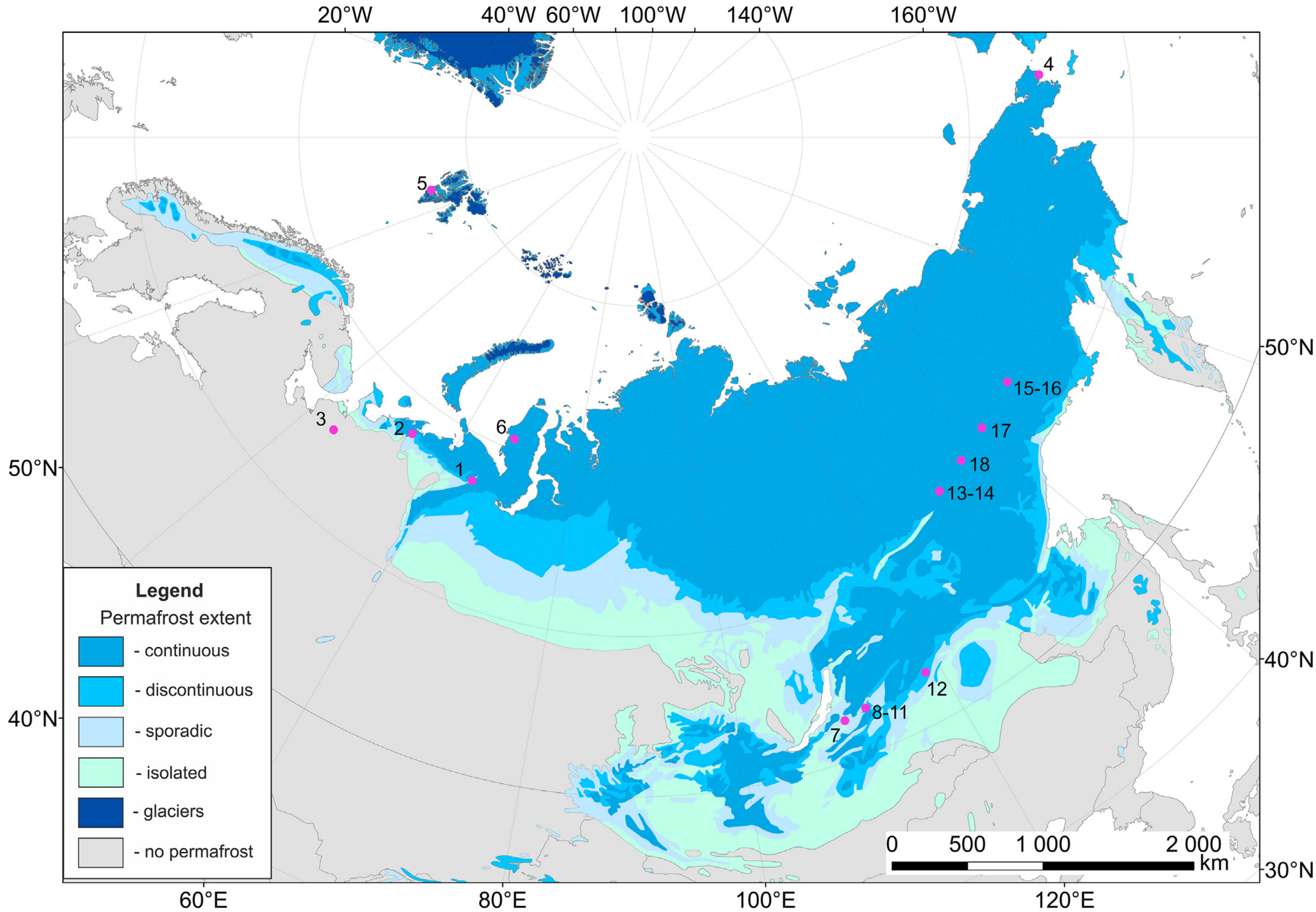

Fig. 1. Location of the study sites and permafrost distribution in Eurasia. 1 ÷ 6: Arctic sites, 7 ÷ 18: ultra-continental sites. See Table 1 for detailed information.

mosses and lichens were removed. To mix air, chamber lids were equipped with fans. Additionally, at the Naryan-Mar and Barentsburg sites (Table 1) we measured the net fluxes of CO_2, CH_4, N_2O, and photosynthetically active radiation (PAR) on plots with preserved natural vegetation, performed in transparent-to-PAR and opaque acrylic chambers 30 × 40 × 40 cm. In this case, a seal was achieved with water locks. Solar radiation intensity (μE s^{-1}) was measured with PAR detector recording data on a HOBO Data Logger (USA). The measurements in transparent chambers took 3 min, followed by 3 min exposure in the opaque chamber. The CO_2 flux rate in the transparent chamber served as an estimate of a net flux of C–CO_2, and in opaque chamber of gross ecosystem respiration. The difference between the two fluxes served to assess the gross primary production.

At the Vorkuta site, net CO_2 fluxes were measured similarly in transparent dark chambers only in human-affected plots and at maximal PAR to assess the difference with soil CO_2 emissions measured simultaneously.

Same chambers were used to sample gas for laboratory measurements of concentrations of methane and nitrous oxide. Air samples were taken by syringe after 1 and 3 h of chamber exposure. Gas samples were injected to vacuum vials and transported to the Laboratory of Gas Chromatography of the Institute of Forest Science (Russian Academy of Sciences). Volumetric concentrations of CH_4 and N_2O were measured on a Kristall 5000.2 (Khromatek, Russia) two-line chromatograph with flame-ionizing and electronic capture detectors. We assume sinks and sources of methane and nitrous oxide in the above-ground vegetation components are negligible, so their estimates of soil emissions are treated as net fluxes.

Thawing depth was measured with a 2 m long and 1.5 cm thick stainless-steel rod. Temperatures of air and soil were estimated with a Checktemp-1 (Hanna Instruments, U.S.) digital thermometer with a stainless-steel probe. Volumetric moisture content in the topmost soil layer was measured with an HH2 Moisture Meter used with an ML2x ThetaProbe soil moisture sensor (Delta-T Devices).

Soil GHG emission measurement points were classified by the effects of human impact on every site. However, both the detailed studies of natural and human controls of soil GHG emissions and areal extrapolations were only made at the Vorkuta site due to the long-term data set and detailed metadata available. Additional ecosystem characteristics included type, composition, and physicochemical properties of the topsoil. Soil bulk density (g cm^{-3}) was assessed in 100 cm^3 monoliths sampled from 0 to 5 and 5 to 10 cm layers, dried to constant mass, and weighed in the lab. Above-ground phytomass estimates in tundra were based on harvests from 0.4 m × 0.4 m plots, and estimates of projected coverage and height of plants by long-term monitoring (1996–2017). Soil trampling was assessed from the known time in which researchers have investigated particular study objects.

Potential microbial respiration fluxes were estimated by the substrate-induced respiration method on disturbed sites. It is widely applied in the lab, but rarely in field conditions. The standard volume of 250 ml of 10 g l^{-1} sucrose solution in distilled water was introduced into soils within the chamber bases. Only microbial respiration, and not the root respiration was stimulated with this treatment (Anderson and Domsch, 1978; Karelin et al., 2017c).

To compare a soil response to moistening in cryogenic ecosystems we also assessed the so-called “Birch effect” (BE) (Birch, 1958), which refers to the CO_2 pulse emission from dry soil after rewetting. The effect was evaluated in field conditions at all the studied sites and micro-sites in the midst of the growing season, during the prolonged periods with the lack of rainfall, when it is most pronounced. This technique was used earlier for the soils of European Territory of Russia (Karelin et al., 2017a). The standard volume of 250 ml of distilled water (equivalent of a 20 mm rain event) was introduced into a soil surface within the chamber bases after routine measurements of basal respiration. After complete water infiltration into the soil, we waited 20 min, and then measured emissions at the new level of soil moisture. The effect was assessed by the ratio of the final to initial CO_2 flux. The 20-min waiting period allows us to estimate a response of microbiota respiration to the water addition until the start of cell division, so it can serve to assess their numbers. According to our estimates, for the chamber base of 95 cm^2, in the upper 6–7 cm of soil, a potential field water capacity was reached.

At every site (Table 1, Fig. 1) along the trans-Siberian, transect Ulan-Ude–Oymyakon, we measured soil CO_2 emissions, methane and nitrous oxide fluxes, the artificial BE, soil temperature and water content, and the depth of the permafrost active layer. Additionally, a vegetation species composition, projected cover, and topography were described, and soil profiles ($n = 12$) were documented and sampled for chemical analysis.

Assessment of CO_2 soil emission at the Lorino site (Table 1) was made for a 55.7 ha settlement area based on fourteen classes of land use recognised on open-access high-resolution satellite images.

2.4. Climate and weather data

For statistical analysis and inter-site comparisons, we used available weather and climate data sets for weather stations from the All-Russian Institute of Hydro-meteorological Information –World Data Centre (RIHMI-WDC, Obninsk, Russia; www.meteo.ru/data), and modelled weather data and the modification of Thornthwaite's Moisture Index provided by Willmott and Feddema (1992), available on-line (WebWIMP, 2009 http://climate.geog.udel.edu/~wimp/wimp map.php).

2.5. Soil characteristics and above-ground phytomass storage

Over 30 soil pits, mostly down to the depth of the permafrost table, were made and documented. Within soil profiles, major horizons were sampled. CHNS determination in soil samples was found using elemental analyser Vario EL cube (Elementar, Germany). Carbon storage in soils was estimated by carbon content in soil horizons and by their bulk density. The database “Characteristics of soils of Northern Eurasia” (Chestnykh and Zamolodchikov, 2018), composed of more than 1800 soil profiles, was used for the sites and plots, where soils were not studied.

The network density of cracks (fissuring of soil) due to cryogenic and desiccation processes was estimated on the soil surface visually or by digital photos. We considered only visually distinguished cracks that were larger than 3 mm in width. Six nominal categories were identified from 0 (no visual cracks) to 5 (total length of visual cracks on 1×1 m of the soil surface >800 cm). The highest crack density was in the haplic vertisol (site 10, Table 1) found in our study and was classified as category 5; intermediate categories were determined linearly.

At every site with tree canopy, the volume of wood in standing trees was estimated on 25×25 m sample plots. These values were converted into storages of above-ground phytomass by regression equations (Zamolodchikov et al., 2005). In the low-canopy biotopes (tundra, steppe, meadow), or in the lower canopy of forest sites the above-ground phytomass of vascular plants, mosses and lichens was cut from the sample plots 40×40 cm, sorted by components, oven-dried, and weighed. In other cases, the values of phytomass components on the sample plots were estimated indirectly using regression equations for the above-ground components of phytomass vs. their partial projective cover (Zamolodchikov et al., 1997). The lack of phytomass storage data was replenished from the database by N.I. Bazilevich (1993).

2.6. Statistical analysis

The statistical analysis was performed with SPSS Statistics V. 20.0 (IBM), PRIMER V. 7 (PRIMER-E Ltd.) and Microsoft Excel. Multiple linear step-wise regression analyses of data available from the Vorkuta site, representing the majority of variables, allowed us to assess the contribution of natural and human impacts to CO_2 emission from soil. For the analysis we introduced three special variables, describing human impact directly: *period of total duration of the disturbance (in years)*, *net duration of the disturbance within the first period (in hours)*, and *recovery period after impact (in years)*. For example, in case of soil trampling, the total duration of the disturbance was 20 years, while the net time of impact is equal to 450 h. The control sites were set to zero durations of human disturbance, and the recovery time was omitted.

Contribution of nominal variables of CO_2 soil emission was assessed with one-way ANOVA. Micro-controls of soil emission along the trans-Siberian transect were analysed by discriminant analysis and principal component analysis (SPSS). Non-parametric distance-based regression analysis (DistLM, PRIMER 6 with PERMANOVA+, PRIMER-E Ltd., UK) was used to estimate the relative contribution of independent variables of CO_2 emission. In that case, a step-wise selection procedure based on the Akaike information criterion was applied to choose the best-fit model.

Unless specifically stated, the non-parametric Mann-Whitney *U* test was used to compare means. The significance level was 0.05.

The regression-based empirical equations (Zamolodchikov and Karelin, 2001; Karelin et al., 2013) were used for calculation and spatial extrapolation of CO_2 net fluxes at the same location in shrub tundra around the Vorkuta site, where we collected data for the models.

2.7. Terms and abbreviations

We use the term “(research) site” to refer to the geographical research locations, as summarised in Table 1 and Fig. 1. The terms “point”, “micro-site”, “biotope”, “habitat”, “local ecosystem”, and “plot” are convertible in the context of the study and serve to identify types and effects of land use or different ecosystems within research sites.

Throughout the text of the study, we treat the human impacts as positive or negative for climate change mitigation. An increase in a sink is positive and an increase in GHG source is negative in relation to the atmosphere according to International Climate policy (Pachauri et al., 2015). Accordingly, the plus or minus signs for fluxes values in the text indicate the sink or source of gas to the atmosphere.

We used means with their standard errors throughout the study. P is a significance level, n is a sample size, r^2 is the coefficient of determination, r_p is the Pearson correlation, and r_s is the Spearman correlation. Soil organic carbon is designated as SOC; other designations are in the text, or trivial.

3. Results and discussion

3.1. Human land use and soil emissions of GHGs in arctic and boreal ecosystems

3.1.1. Analysis of CO_2 soil emission controls with land use

Fig. 2 combines all available field observations of CO_2 soil emission in 2014–2017 at the stationary sites (1–6) affected by human land use. As we found, almost any local human impact inevitably results in either an increase or reduction in CO_2 soil emission, as compared to unaffected (natural) ecosystems. Only in 3 out of 29 cases presented on the diagram, were the affected carbon dioxide fluxes from soil not significantly different from natural rates ($P > 0.05$). Another significant conclusion we could draw was the increase in soil CO_2 emissions in most cases of local human impacts. The extent of this growth outpaced the extent of decrease in cases, where the CO_2 emissions fell. Therefore, acting together, human land use factors commonly resulted in greater mean and variance in soil CO_2 emission, proportional to its initial (natural) rate. This was found in tundra (0.110 ± 0.03 (land use) > 0.077 ± 0.01(natural) g C m^{-2} h^{-1}, $P < 0.05$) and northern taiga (0.166 ± 0.04 (land use) > 0.123 ± 0.02 (natural) g C m^{-2} h^{-1}, $P < 0.05$). Some land use controls (the "embankment effect", (f)) could increase primary production of vegetation and hence enhance below-ground respiration of roots and rhizospheric microbiota, whereas another ("trampling", (b)) would decrease soil CO_2 emission. However, according to our field estimates under optimal PAR conditions, in most cases they result in a shift of the balance to net C-source to the atmosphere. This is mostly due to elimination of vegetation (primary production), which is commonly derived from human land use. The most common combination was soil trampling and increased thaw depth. It usually caused a decrease in soil CO_2 emission. Emission losses in the upper soil layer due to destruction of vegetation cover were not offset by increased emission from the thawing permafrost in deeper soil layers.

Human impact was most extensively examined in the southern shrub tundra zone at the Vorkuta site where the impact on soil CO_2 emission variations was the highest according to regression analysis (Table 2). *Total net time of land use* (standardized regression coefficient $\beta = +0.36$) and negative effect of the *recovery time* ($\beta = -0.25$) were among the factors that contributed most. This suggests that the human impacts stimulated the emission, although during the ecosystem recovery the emission dropped to the initial level. When autumn data were considered (July–September, Table 2), the contribution of the second variable became negligible, and predictive power of the model slightly decreased. Significant natural CO_2 emission factors included *thaw depth* ($\beta = +0.53$), *above-ground phytomass storage* (+0.38), *thickness of the top organic layer* (+0.21), and *air temperature* (+0.17).

All variables except for the *recovery time* were positively linked to emission. It should be noted that natural independent variables were also partially controlled by human impacts. For example, the above-ground phytomass storage was negatively correlated with soil bulk density in the 0–5 cm range ($r_p = -0.59$, $P < 0.01$) (Fig. 3), whereas the latter was positively linked to trampling intensity. Thawing depth experiences logarithmic growth with soil trampling, which becomes evident after a total disturbance time of approximately 100 human-hours (Fig. 4). When thawing depth increased twofold compared to the initial state, it would not recover and soil in winter did not freeze down to the permafrost table. Thawing depth remained greater on post-fire sites (Fig. 5; paired Tukey's test, $P < 0.05$). Air and soil temperatures were higher in the waterlogged ditches running along the railroad subgrade elevations and inside the settlements, and lower for barren soil, compared to natural tundra sites. Hence, the real contribution of human impact actors is even higher than the regression analysis showed.

Note that the most significant drivers of soil CO_2 emission in the intact tundra at the same site during the vegetation season were *soil temperature at 5 cm*, *air temperature in the plant canopy*, *thaw depth,* and *above-ground phytomass storage* (Karelin and Zamolodchikov, 2008).

The same data sets were treated with one-way ANOVA to account for nominal soil emission factors. *Biotope type* (sixteen local ecosystems with various impacts) and *soil topmost composition* (automorphic or hydromorphic regimes, gravel, cultural layer) were among the significant variables. Post hoc paired comparisons in significant variable categories

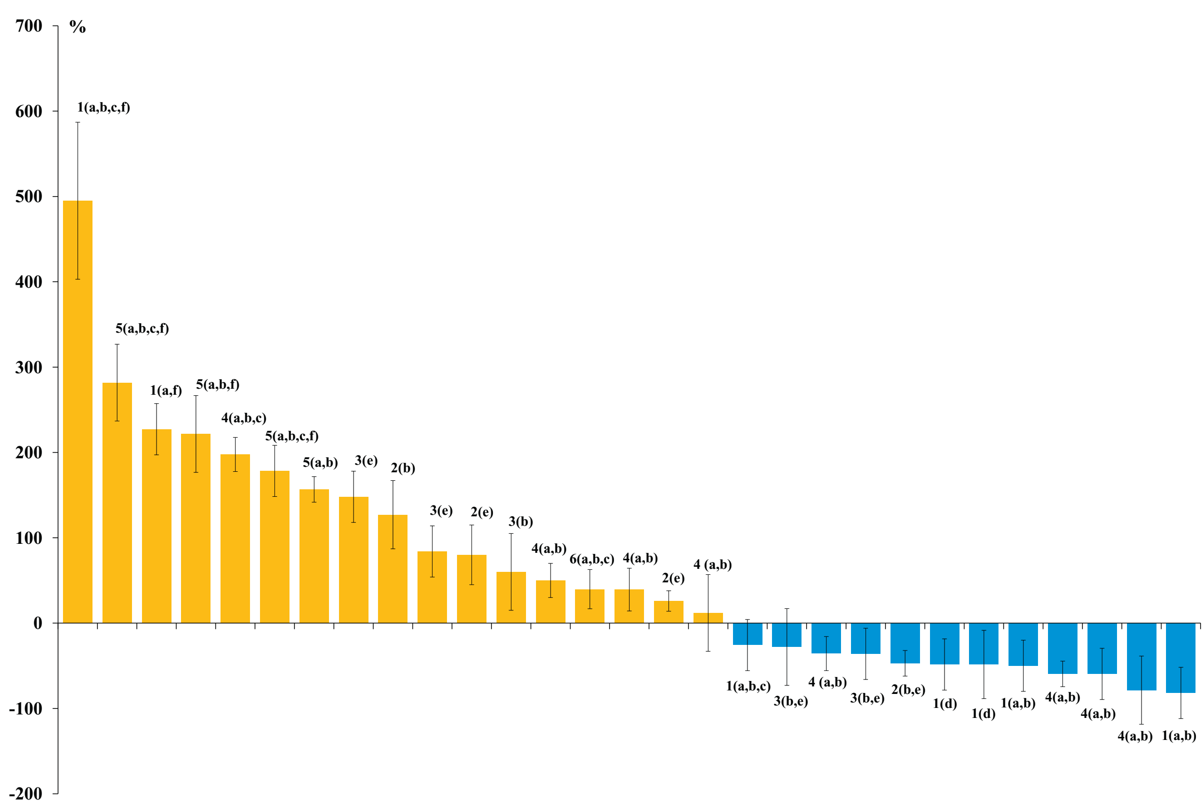

Fig. 2. Change in soil CO_2 emission rates in the studied arctic ecosystems affected by land use (29 micro-sites included). Every bar represents a site with specific effects of land use (numbers correspond to the sites in Table 1; letters correspond to land use effects in Section 2.2). Bars are ranked in descending order. Orange bars – increase in soil emission (%), blue – decrease (%), as compared to natural analogues. Means and standard errors are given ($n = 10 \div 45$).

Table 2
Multiple linear step-wise regression analysis of CO_2 emission from human-affected soils in shrub tundra (Vorkuta site, 2014).[a]

Period of observations	Model	Standardized coefficients β of significant independent variables	Excluded variables	r^2	n
July–August	$8.89.\ 10^{-8}$. ANSUM – 0.001· ANREST +0.00038·PERM +0.0046. TA + 2.08. 10^{-5}. PHYTO + 0.005. SOIL – 0.079	PERM (0.53), PHYTO (0.38), ANSUM (0.36), ANREST (−0.25), SOIL(0.21), TA (0.17),	T_1, T_{10}, ANTOT, DENS, SM, MOS	0.89	61
July–September	$1.19.\ 10^{-7}$. ANSUM + 0.00028. PERM + 0.0031. TA + 6.43. 10^{-6}. PHYTO + 0.008. SOIL – 0.058	ANSUM (0.47), SOIL(0.34), PERM (0.30), TA (0.22), PHYTO (0.14)	T_1, T_{10}, ANTOT, ANREST, DENS, SM, MOS	0.70	138

[a] Dependent variable: CO_2 efflux from soil ($g\ C \cdot m^{-2} \cdot h^{-1}$). Independent variables: TA – air temperature at 30 cm (°C), T_1 – soil temperature at 1 cm, T_{10} – soil temperature at 10 cm, SM – volumetric soil moisture in 0–7 cm (%), ANTOT – "end of influence – start of influence": total period of land use (yr.), ANREST – time since termination of land use, "restoration period"(yr.), ANSUM – total net time of land use (h), PERM – thaw depth (cm), PHYTO – above-ground phytomass storage (a.d.w, $g\ m^{-2}$), MOS – thickness of moss-lichen layer, cm, SOIL – thickness of topmost organic layer, cm, DENS – soil bulk density in 0–5 cm, $g\ cm^{-3}$. Both models are significant at $P < 0.001$. All regression coefficients are significant at $P < 0.001$, PHYTO ($P = 0.007$).

showed that all types of human impact cause change in the emission level compared to the control ($P < 0.05$). The most pronounced difference of mean efflux rates between biotopes was found in railroads and drained intact tundra ($P < 0.001$). The CO_2 emission rate in hydromorphic tundra and waterlogged biotopes differed significantly from each other ($P < 0.05$). Soil composition had the largest effect on the emission when hydromorphic soil was replaced with gravel ($P < 0.001$). *Meso-relief* (upland, depression, slope) was insignificant ($P = 0.65$).

We attempted to assess a relative quantitative contribution of individual CO_2 emission factors using DistLM on the same dataset. It showed mainly similar links with only slight differences. When July–September (Table 3) data were considered, the model described 65% of total variance. The main factors remained the same: *total net land use time* (33.2% of total variance:), *topmost organic layer thickness* (12.4%), and *thaw depth* (9.9%). The remaining variance was described by *soil temperature at depth of 10 cm* (4.7%) and *above-ground phytomass storage* (3.4%). Air temperature and soil bulk weight were insignificant. Hence, land use factors explain a third of the total variance.

When only summer months July and August were taken into account, the model had higher significance (70% of total variance), with decreased contribution of human impact (*total net time of land use* 9.2%), and increased input of *thaw depth* (30.4%), *phytomass storage* (9.2%), *soil bulk density* (3.6%), *soil moisture* (3.3%), and *air temperature* (2.2%).

3.1.2. Substrate-induced soil respiration with land use

The multiple linear regression of substrate-induced CO_2 flux from soil has demonstrated a high coefficient of determination (Table 4: $r^2 = 0.75$, $P < 0.001$). The most important difference with the analogous model in Table 2 is the lack of significant land use variables. Addition of the minimal amount of sucrose to stimulate microbial respiration reduced the effects caused by land use factors. This supports the suggestion that land use controls suppress not only the root, but also microbial respiration. Suppression of soil respiration was mainly caused indirectly by destruction of above-ground phytomass, and directly through physicochemical alterations in affected soil by its change to gravel and sand, trampling, fires, and abiogenic or biogenic subsidies. Moreover, the set of significant variables in this case varies or the nature of the relationship with a particular variable could change, as in the case with the depth of thaw. Positive links were found with *initial rate of CO_2 emission* and *organic layer thickness*, negative links with *soil moisture*, *thawing depth*, and *soil bulk density*.

Dynamics of soil respiration significantly differed in human-modified biotopes after addition of sucrose solution and two patterns of response were observed. The first was similar for intact biotopes. Respiration rate rapidly grows during 1–3 h after addition of sucrose solution and then gradually decreases. The shape of curves shows that stimulating effect vanishes in 3–4 days. The second set of measurements on the same points 53–56 days after did not show any difference with a new control plots (t-test, $P = 0.17 \div 0.89$).

The substrate-induced increase in respiration was the most pronounced at the old post-fire sites dominated by mosses (*Polytrichum juniperinum* L.), which prevented the development of a root layer by outcompeting vascular plants. This implies that the main component of soil respiration and gross respiration was the microbial respiration. We have concluded that fires affected the composition of soil microbial community via the effects on vegetation and thawing depth.

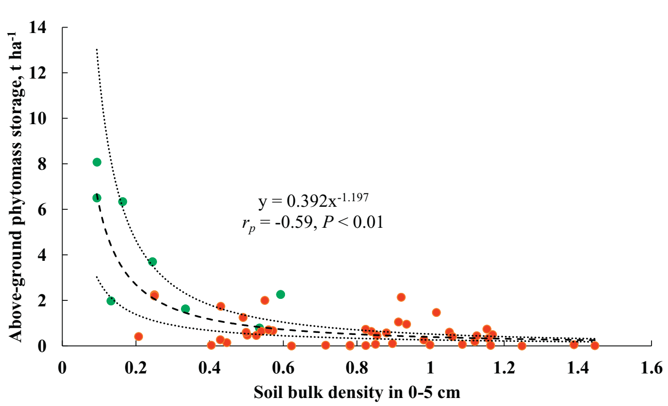

Fig. 3. Aboveground phytomass storage ($t\ ha^{-1}$ a.d.w.) vs. soil bulk density in 0–5 cm layer ($g\ cm^{-3}$) in shrub tundra. Green markers are natural ecosystems; red markers are human-effected sites (Vorkuta site). The regression line is a power function with 95% upper and lower confidence bands ($n = 103$).

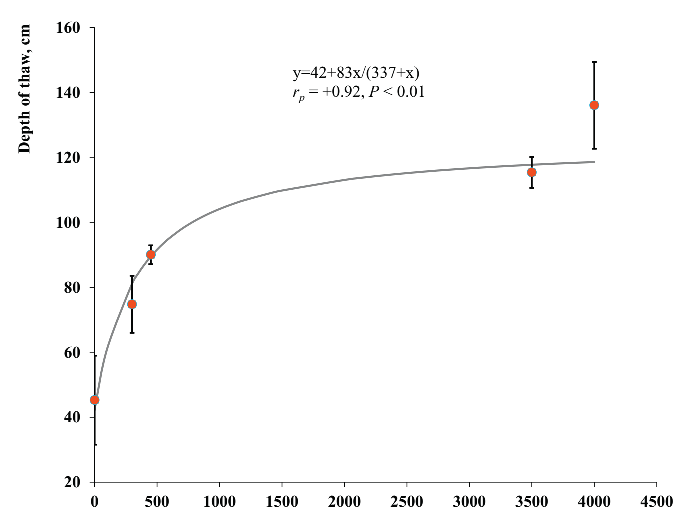

Fig. 4. Thaw depth vs. sum of trampling in human-affected tundra sites (Vorkuta site). The regression line is hyperbolic. Means and standard errors are given ($n = 20 \div 484$).

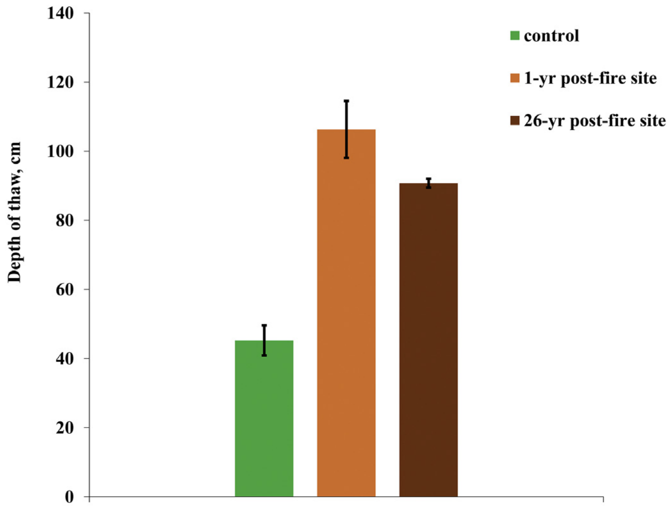

Fig. 5. Maximal seasonal thaw depth at undisturbed tundra sites (control) and post-fire biotopes of different ages (Vorkuta site, 2016). Means and standard errors are given ($n = 80$).

The second type of dynamics of slow increase or even slight decrease in SR during the first 1–3 h, followed by fast increase, was specific for human-affected biotopes. It was observed in biotopes with pronounced soil trampling and was related mainly to constrained percolation into dense soil. On the one hand, such an effect could be treated as a technical artefact. However, it demonstrates the consequences of soil trampling, limiting precipitate or dust input of biogenic elements to ecosystems.

The factors of CO_2 emission after addition of sucrose were evaluated, as previously, by DistLM. However, in this case an independent nominal variable of *occurrence of fire* (1–26 years ago) was introduced. The addition of sucrose was shown to remove limitations set by human impact on microbial communities, making it insignificant (Table 5). However, post-fire sites demonstrated markedly high contribution to total variance (25.8%), which suggest that other features of fire disturbance were not accounted for in our equations like severity of fire or quality of fire fuels.

3.1.3. Upscale: Joint action of land use controls on CO_2 emissions from soil on larger areas

We assessed the cumulative effect of land use for larger areas of high human impact (coalmining infrastructure; land use effects a, b, c, and f, occupying 100% of 0.5 km^2 and moderate human impact (land use effects a–f, occupying 14.8% of 3 km^2) in the southern shrub tundra at the Vorkuta site.

The Yur-Shor coalmining complex at the Vorkuta site was filled in 20 years ago (1999) and recultivated several years later. Despite the remediation of the disturbed area of 0.5 km^2, the average flux measured during the culmination of the growing season in August 2016 was significantly higher than in intact tundra of the same area. September measurements further increased the difference due to faster seasonal decline in SR in intact tundra than on disturbed micro-sites (Fig. 6).

This could be attributed to the constantly elevated soil temperatures on the mine territory during August and September, as compared to native tundra (+9.5 > +6.3 °C (at the depth of 10 cm), $P < 0.05$). This difference is due to lack of permafrost and accumulations of industrial black carbon and dust. Another reason is a continuously high CO_2 emission from the bore of the mine shaft, which was filled with concrete 20 year ago. Despite the closure, it still contributed 8.4% to CO_2 emission from the mine territory, while occupying only 0.7% of its area. Higher contribution of non-rhyzospheric soil microorganisms on the territory of the mine during autumn could also serve an explanation.

CO_2 fluxes from the closed coalmine shaft (+4.81 g C m^{-2} h^{-1}) and emission from the dirt road measured right after a vehicle passage (+2.84 g C m^{-2} h^{-1}) were recorded as the highest sources (Fig. 7). These values were an order of magnitude more than other sources in human-affected ecosystems in Arctic and boreal domains (Karelin et al., 2017b). Only the localization of these highly intensive sources limits their significance in the cumulative emissions from the human impact areas. Nevertheless, their contribution made the modified tundra of the mine complex a much higher source than the intact tundra of the same area. Applying our empirical regression equations of net carbon fluxes in tundra (Zamolodchikov and Karelin, 2001; Karelin et al., 2013) to weather conditions and phytomass storage in 2016, showed that surrounding tundra was a weak sink of -19 ± 12 g C m^{-2} yr^{-1}, while the Yur-Shor mining complex acted as a strong net source of $+755 \pm 45$ g C m^{-2} yr^{-1}. Therefore, despite the fact that for many years the mining complex remained unmanaged, its area of 0.5 km^2 emitted the same amount of carbon as was absorbed by 20 km^2 of intact tundra.

Intensive emission of CO_2 from dirt roads induced by vehicle loads was never described quantitatively. Similar to other types of mechanical loads on the soil profile, the atmospheric flux is formed by desorption of older CO_2 from the soil particles under external pressure after unburdening (Smagin et al., 2016). Without loading, the same amount can be stored in soil for a long time. The replenishing mechanism for this flux is the lateral diffusion within the soil profile. This was one of the strongest sources acting in tundra rapidly within several hours (Fig. 7). As shown, the higher the load is, the greater the emission rate is, likely due to the involvement of the older carbon, which does not participate in the rapid diurnal or seasonal carbon exchange driven by plants.

The contribution of different land types to cumulative emission from landscapes was also estimated under moderate human impact (Fig. 6). The area of interest in the southern tundra was equal to 3 km^2 and included most of the land use effects (a–d, f), occupying together 14.8% of the area. The spatial distribution of the biotopes taken from a Landsat image (Google Earth, July 30, 2013) and application of our field

Table 3
Non-parametric distance-based regression analysis (DistLM) of relative contribution of factors of CO_2 emission from human-affected soils in shrub tundra (Vorkuta site, 2014).[a]

Independent variables	Resulting Akaike Information Criterion	Pseudo-F criterion	*P* (significance level)	Proportion of variance explained by each variable	Cumulative proportion of variance explained by included variables	Degrees of freedom
ANSUM	−1164.7	82.573	0.001	0.33205	0.33205	189
SOIL	−1200.1	40.713	0.001	0.12388	0.45593	188
PERM	−1234.5	39.178	0.001	9.9092E-2	0.55703	187
T_{10}	−1252.4	20.42	0.001	4.6789E-2	0.60482	186
PHYTO	−1278.6	17.267	0.002	3.414E-2	0.63819	184
DENS	−1279.4	2.7407	0.11	5.3682E-3	0.64256	183
TA	−1279.9	2.402	0.132	4.669E-3	0.64822	182

[a] Dependent variable: CO_2 efflux from soil. For abbreviations of independent variables, see Table 2. Significant variables are in bold. Initial set of independent variables is identical to Table 2.

Table 4
Multiple linear step-wise regression analysis of CO_2 emission from human-affected soils in the southern shrub tundra (Vorkuta site, July–August 2014) after standard addition of sucrose solution.[a]

Model (in parentheses are significance levels of regression coefficients)	Standardized coefficients β of significant independent variables	Excluded variables	r^2	n
1.06. FLUX (<0.001) – 0.00047. PERM (<0.001) – 0.0011. SM (<0.001) – 0.042. DENS (0.015) + 0.0063. SOIL (0.016) + 0.193 (<0.001)	FLUX(0.61), SM(−0.34), PERM(−0.25), SOIL(0.2), DENS(−0.16),	ANSUM, ANTOT, ANREST, TIME, T_1, T_{10}, TA, PHYTO, MOS	0.75	82

[a] Dependent variable – substrate-induced CO_2 efflux (g C m^{-2} h^{-1}) after addition of sucrose solution. Independent variables: FLUX – initial CO_2 efflux from soil before addition of sucrose (g C m^{-2} h^{-1}), TIME – time after addition of sucrose solution, min. Other variables abbreviated in Table 2. Model is significant at $P < 0.001$.

Table 5
DistLM of relative and absolute contribution of factors of CO_2 emission from human-affected soils in shrub tundra (Vorkuta site, July–August 2014) after standard addition of sucrose solution.[a]

Independent variables	Resulting Akaike Information Criterion	Pseudo-F criterion	P (significance level)	Proportion of variance explained by each variable	Cumulative proportion of variance explained by included variables	Degrees of freedom
FIRE	164.44	39.365	0.001	0.25836	0.25836	113
FLUX	160.41	6.0241	0.028	3.7854E-2	0.29621	112
SM	151.28	11.282	0.002	6.4931E-2	0.36115	111
SOIL	147.47	5.7078	0.023	3.1514E-2	0.39266	110
PHYTO	142.39	6.915	0.009	3.6232E-2	0.42889	109
ANREST	140.48	3.7339	0.065	1.9085E-2	0.44798	108

[a] Dependent variable – substrate-induced CO_2 efflux. FIRE – presence of fire (1–26 years ago) in a site history. For abbreviations of other independent variables, see Tables 2 and 4. Significant variables are in bold. Initial set of independent variables is identical to Table 4.

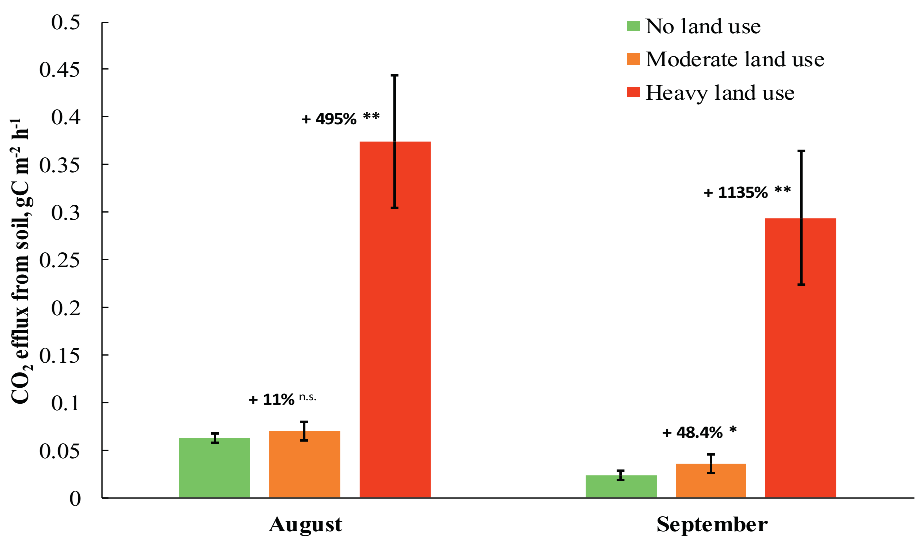

Fig. 6. CO_2 soil efflux from territories at the Vorkuta site with moderate, heavy, and no human land use pressure (August–September 2016). Means and standard errors are given ($n = 40 \div 215$). Differences with soil flux from natural tundra landscapes (no land use) are in per cent: $^{*}P < 0.05$; $^{**}P < 0.001$.

estimates of soil emissions showed that at the peak of the vegetation season this human-modified landscape emits 11% more than intact tundra of the same area. However, similar to the high human impact plot, with the onset of the cold season (end of September) the contribution of the human-modified biotopes significantly increased (Fig. 6: +48.4%). This was due to the modified ecosystems showed a markedly lower seasonal decrease in SR compared to natural habitats. Of all the habitats affected by human activities, the most significant contribution to total emissions from this area was made by railroad-affected habitats.

Thus, both levels of human land use impact on a landscape demonstrated similar autumnal growth of contribution of the human-modified ecosystems to CO_2 soil emission. However, in winter, the emission almost solely depends on the snow cover thickness (Karelin and Zamolodchikov, 2008); hence, without winter measurements it is hard to predict the future course of events. It is clear that the land use contribution to soil respiration differs in the annual cycle, and winter emissions are essential for adequate assessment.

At the Lorino site (Table 1), in August–September 2013 we estimated efflux from soils throughout the territory of a typical seaside native settlement of Chukchi and Eskimo tribes in the Arctic (Lorino, 55.7 ha, 900 habitants). Preliminary measurements allowed identification of fourteen land use types over the territory of the settlement (namely, boiler stations, different building types, utilities network, dirt roads and sites, wastelands). Measured values of soil respiration varied from $+0.034 \pm 0.009$ g C m^{-2} h^{-1} on sandy abrasive slopes of the settlement to $+0.43 \pm 0.01$ g C m^{-2} h^{-1} under the buildings not contacting permafrost, but with no equipped ventilated cellar, and even $+1.48$ g C m^{-2} h^{-1} under cages of an arctic fox fur farm. Across the buildings, the soil respiration grew with the heat impact of the building on the soil; buildings with cold ventilated cellars had 5–6

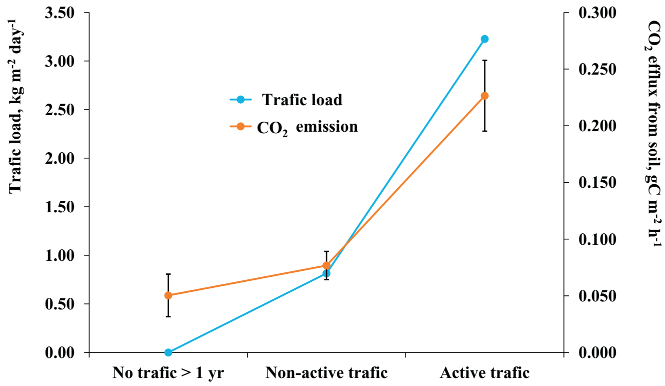

Fig. 7. Effect of traffic load in shrub tundra landscape on CO_2 emission from gravel roadbeds. Means and standard errors are given (Vorkuta site, $n = 106$). The traffic load was estimated by the average weight of loaded cargo tracks and visual frequency of traffic per day.

times less respiration compared to the primary forms of permafrost isolation. The total CO_2 flux average weighted by land use type areas was estimated at $+0.168 \pm 0.076$ g C m^{-2} h^{-1}, or 40.3 kg C ha^{-1} d^{-1}. Taking into account that vegetation cover inside the territory of the settlement is negligible, we can assume that the observed emission rate corresponds to the net C flux, if not considering additional emissions from local fuel burning, and other activities.

We can compare this amount with the carbon balance previously estimated for a typical tundra landscape in adjacent area (40 km away, vicinities of Lavrentiya village; Zamolodchikov et al., 2003). During the same season (August–September), tundra was acting on average as a carbon sink of -5.1 g C m^{-2}, which is equal to -0.9 kg C ha^{-1} d^{-1}. Taking the emission estimate of 40.3 kg C ha^{-1} d^{-1} for the average flux in August–September, it is easy to calculate that to assimilate the emitted amount of C from the settlement during the same period, it needs 46.6 times more intact tundra. However, if compared with a more balanced by C exchange territory of tundra, it increases the area needed for assimilation of the emitted carbon many times over. Additionally, this emitted amount is derived only from soil respiration, and it does not include direct carbon emission from local fuel burning. According to our unpublished estimates of the local carbon footprint (Gleb N. Kraev, personal communication, September 20, 2018), soil respiration comprises up to 16.5% of annual CO_2 emissions in the village territory, whereas local fuel burning alone contributes another 70.5%.

3.1.4. Methane and N_2O fluxes with land use

Anthropogenic factors strongly affect all major biogenic GHGs, but this influence is different. Whereas, soil emission and CO_2 efflux to the atmosphere would normally rise with land use, thereby providing a conventionally negative environmental effect, the effect of local land use on methane flux is mostly mediated by the influence of soil moisture via human-induced drainage (land use effects a, b) or waterlogging (f) ($r_p = +0.73$, $P < 0.01$; Fig. 8). In most cases, this is common for tundra ecosystems under various studied types and effects of land use. Depressions in meso-relief, which serve as CH_4 sources ($+0.64 \pm 0.35$ mg CH_4 m^{-2} d^{-1}), became weaker sources (from $+0.10 \pm 0.04$ to $+0.20 \pm 0.02$), or sinks (-0.15 ± 0.02) under land use. Automorphic elevations in meso-relief remain similar (-0.22 ± 0.09 and $-$ 0.16 ± 0.02, $P > 0.05$), or stronger sinks of methane (-0.44 ± 0.04 (1-yr old post-fire plot), -0.39 ± 0.02 (railway subgrade). Methane fluxes were not significantly differed from zero only in three out of fourteen types of biotopes. Hence, human impact tended to weaken methane sources, or to increase the sinks (positive effect for the atmosphere).

The addition of methane fluxes from human-affected biotopes decreased the total response of 3 km^2 of shrub tundra landscape ($+0.207 \pm 0.14 > +0.161 \pm 0.12$ mg CH_4 m^{-2} d^{-1}, $P < 0.05$). The area-weighted methane flux was even lower ($+0.065 \pm 0.037$ mg CH_4 m^{-2} d^{-1}, $n = 48$) on 0.5 km^2 of coal mining complex with more intensive human impact. Even though the strong flux from the coalmine shaft filled with concrete ($+76.9 \pm 30$ mg CH_4 m^{-2} d^{-1}, $n = 6$; the area of the shaft was 962 m^2) would seriously increase the area-weighted flux up to $+0.601 \pm 0.037$, this flux includes methane from deep layers, not affected by the surficial processes like draining.

Sinks of methane and nitrous oxide are also observed in the surface atmospheric layer, which is possibly due to light-induced methane oxidation by hydroxide, and photolysis and fixation of nitrous oxide by bacteria in above-ground vegetation. However, little is known on the related specific processes occurring in the surface air and vegetation (Marushchak et al., 2011, 2016; Oertel et al., 2016). Nevertheless, the sinks of both gases were repeatedly recorded in typical tundra peat complexes in transparent-to-PAR chambers with vegetation in daylight conditions at Naryan-Mar site (Table 1).

Similar data on GHGs could be found in other studies. Drainage of Arctic territories increased soil emissions of CO_2 and N_2O, but decreased methane fluxes (Petrescu et al., 2015). Both sources and sinks of methane in tundra during the vegetation period were frequently evidenced. The balance of methane fluxes on the soil surface is controlled by joint activity of anaerobic methanogens as CH_4 producers, and methane oxidizing aerobic methanotrophs in the topmost soil, as consumers. The ratio of these processes forms either a source or sink of the gas to the atmosphere (Curry, 2007). In our study, intact shrub tundra mostly acted as a methane source ($+0.207 \pm 0.14$ mg CH_4 m^{-2} d^{-1}, $n = 30$), whereas human-affected sites were sinks (0.108 ± 0.05 ($n = 52$)).

Soils in intact northern taiga biotopes (Pinega site, Table 1) in mature coniferous forests dominated by Scots pine or Norway spruce were sinks of -0.302 ± 0.08 mg CH_4 m^{-2} d^{-1} ($n = 18$). Boreal wetlands were sources of $+0.209 \pm 0.06$ ($n = 3$). Human-affected ecosystems (mowed meadows, vegetable gardens) demonstrated zero-balanced methane fluxes (-0.071 ± 0.076; $n = 12$).

The average methane (-0.081 ± 0.112 mg CH_4 m^{-2} d^{-1}, $n = 8$) and nitrous oxide fluxes ($+0.082 \pm 0.096$ mg N_2O m^{-2} d^{-1}, $n = 8$) were close to zero ($P > 0.05$) in intact and human-modified (land use types: a–f) polygonal patchy arctic tundra (Barentsburg site, August 2017). A significant methane sink increase (-0.172 ± 0.049 mg CH_4 m^{-2} d^{-1}; $P < 0.05$) was only found on vegetated coalmining slagheaps and dumps. The control biotopes of polygonal tundra tended to be either weak sinks on the dryer polygons or sources in moist polygonal cracks or in micro- and meso-depressions, resulting in near zero landscape methane balance (-0.075 ± 0.28 mg CH_4 m^{-2} d^{-1}).

Contrary to methane, land use mostly stimulated soil N_2O emissions in tundra. Nevertheless, the nitrous oxide fluxes were near zero in six out of fourteen biotopes, including the automorphic control tundra. The largest source of nitrous oxide ($+1.17 \pm 0.27$ mg N_2O m^{-2} d^{-1}) was found in the automorphic habitat with moderate trampling. The only significant sink (-0.33 ± 0.25) was found in the moderately trampled hydromorphic biotope.

Mechanisms involved in the soil N_2O sink remain understudied. A similar study also reported both sinks and sources of N_2O in Svalbard arctic tundra (Chen et al., 2014). Moreover, significant absorption of N_2O (-0.19 mg N_2O m^{-2} d^{-1}) was measured in our study in depressions with dark chambers over preserved vegetation compared to the near zero balance of a flat surface in elevated peat polygons (typical tundra, Naryan-Mar site, Table 1). Furthermore, absorption of N_2O increased in both micro-sites when exposed to light.

There was evidence of a weak gas sink (-0.307 ± 0.203 mg N_2O m^{-2} d^{-1}) in intact lichen pine forests, but a source in various spruce forests ($+0.171 \pm 0.14$, $n = 9$) in northern taiga. Landfills in the pine forests significantly enhanced the nitrous oxide emission ($+1.92 \pm 0.32$, $n = 12$).

Area-weighted fluxes of nitrous oxide were significantly higher, when the land use biotopes were considered for a 3-km^2 plot of shrub

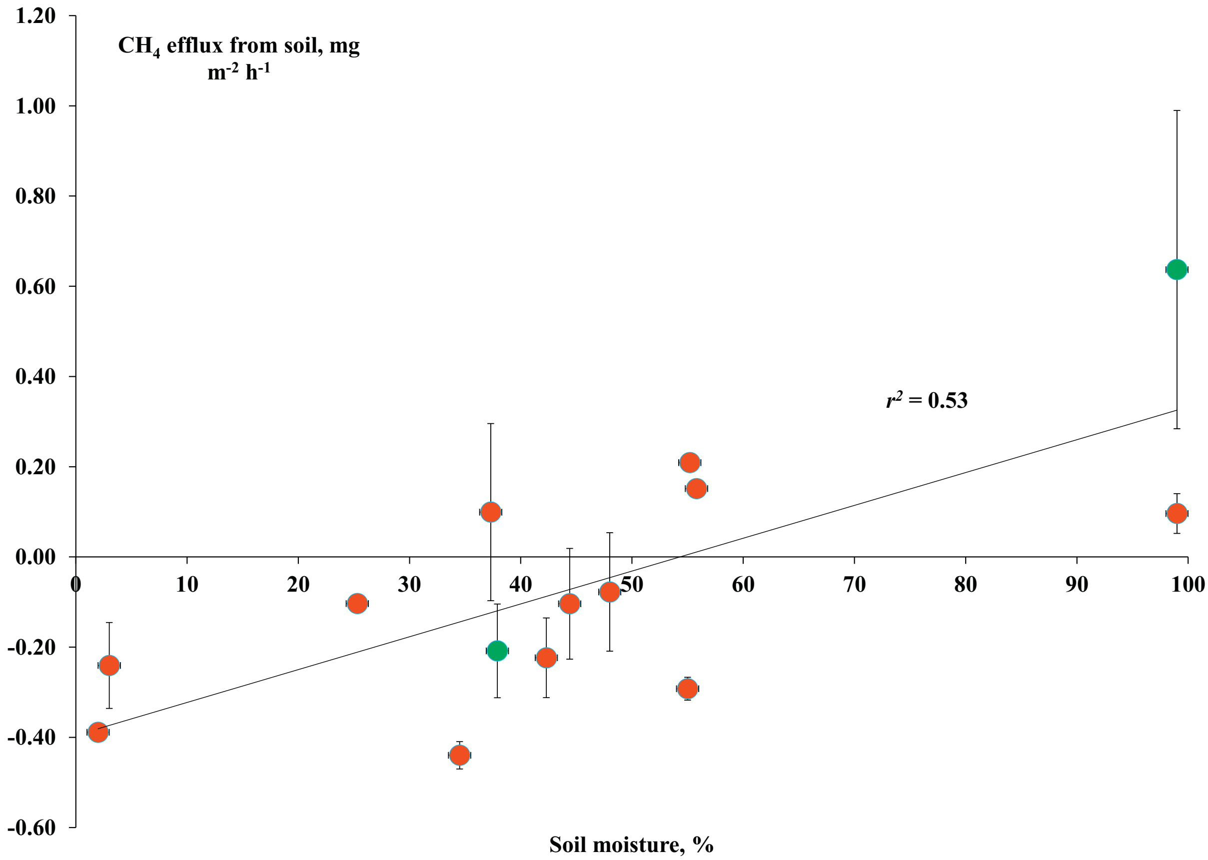

Fig. 8. Methane fluxes in natural (green dots; lower green dot – micro-elevations, upper – micro-depressions) and human-affected (red dots) biotopes in shrub tundra (included effects of land use are (a), (b), (d) and (f) at Vorkuta site and (a), (b), (d), (e) at Naryan-Mar) vs. volumetric soil moisture in 0–7 cm (%). Negative values are methane net sinks from the atmosphere, positive – net sources. Means and standard errors are given.

tundra at the Vorkuta site ($+0.041 \pm 0.015 < +0.144 \pm 0.1$ mg N_2O m^{-2} d^{-1}, $P < 0.05$).

Our eastern European nitrous oxide flux estimates in shrub tundra fall in the range of -0.009 to $+10.4$ mg N_2O m^{-2} d^{-1} previously estimated for the same local region (Marushchak et al., 2011). However, our methane flux estimates excluding the coalmine case were significantly lower than the corresponding range of $+1.9$ to $+10.1$ mg CH_4 m^{-2} d^{-1} by Berestovskaya et al. (2005) and Marushchak et al. (2016) for intact shrub tundra. This is likely a consequence of the human impact at the Vorkuta site, and a bias due to dominant interest of the researchers to lowland micro-sites.

3.1.5. Comparison with published data on the effect of land use on GHGs fluxes in the Arctic

Little evidence on the effect of land use on the three GHGs supports our findings. Intensive reindeer grazing was followed by an increase in soil temperature and altered sensitivity of microbial community to it, and thus modified CO_2 emissions (Stark et al., 2015). In this study, SR at lower temperatures was lower at the sites with intensive grazing than in moderately disturbed sites due to weaker thermal insulation caused by destruction of soil and vegetation cover. The microbial community species composition also changed. Grazing as any type of mechanic destruction of thermal insulation was shown to decrease the microbial ability to acclimate to low temperature by changing the slope of respiration–temperature relationship (Q_{10}). It was suggested that suppression of microbial respiration by low temperatures could surpass its stimulation by reindeer faeces as organic fertilisers. Our estimates showed that grazing not only suppresses SR on sands and loams in tundra (Naryan-Mar site; $0.085 \pm 0.011 > 0.045 \pm 0.006$ g C m^{-2} h^{-1}, $P < 0.05$), but also stimulates it on peatland pastures ($0.071 \pm 0.008 < 0.107 \pm 0.026$ g C m^{-2} h^{-1}, $P < 0.05$), thus supporting the significance of soil and micro-topography. Importantly, semi-domestic reindeer grazing or other human impacts damaging soil and vegetation covers could affect soil microbial respiration not only mediated by vegetation, but also directly through soils.

A review of biogenic GHG exchange with the atmosphere in arctic, boreal, and temperate wetlands (Petrescu et al., 2015) showed that drainage and exploitation of natural wetlands had positive feedbacks for the greenhouse effect owing to growth of CO_2 and N_2O emissions, despite the decrease in methane emissions. This agrees absolutely with our data: local cumulative action of land use factors supports growth in net emissions of CO_2 and N_2O, and decline in CH_4 emissions in arctic and boreal ecosystems.

Soils of modified ecosystems on Svalbard, including abandoned coalmines, slugheaps, dumps, and settlements, were shown to have significantly higher summer emission of CH_4 and N_2O than intact arctic tundra, and even ornithogenic soils (Chen et al., 2014). Intact moist tundra could be either source or sink of these gases. Flux rates and human-induced emphasis of N_2O fluxes were controlled by soil ammonium concentration and were comparable to our estimates. It was suggested that local human impact contributed more than climate change to soil respiration in the Arctic.

We were able to test this hypothesis for soil CO_2 emissions with our field estimates and regression modeling. Using our empirical regression equations for carbon fluxes (Karelin et al., 2013) and known input of SR to gross ecosystem respiration (Karelin and Zamolodchikov, 2008) we assessed the relative contribution of human impact and climate change for southern shrub tundra at the Vorkuta site. Soil CO_2 emissions during the vegetation season (May–September) were estimated to increase by 79.3% during the warming period of 1996–2014. Estimates made in this study show that land use controls promote the increase in the emission over that territory by 11–48.4%. Time frames of 21 years (1996–2014) were clearly set in the first case; however, it was impossible to set them exactly in the second case owing to different types and durations of human impacts. However, most human impacts on the studied territory occurred during 1988–2014, which is comparable to the period of climate change assessment. Thus, we can conclude that human impact and contemporary climate warming have produced similar effects on CO_2 emissions from cryogenic soils locally for at least two decades.

3.2. Ultra-continental extreme environment and GHG soil emissions

3.2.1. Macro- and micro-ecological factors of CO_2 efflux from soil

There is no agreement on the Arctic limits within the cryolithozone. Conventionally, the Arctic includes mainly open landscapes of tundra on permafrost. Such areas are subject to the effect of the ocean and comprise the lesser part of the permafrost zone. Ultra-continental lands occupying large areas in central and northeastern Eurasia (Fig. 1) are covered by taiga, dominated by larch forests. Compared to the Arctic zone, permafrost reaches maximal thickness of 1370 m, with average of 300–500 m in Central Yakutia. Additionally, the coldest soils in the Northern Hemisphere are found there (Savvinov, 1976). There are mostly isolated patches of much thinner permafrost in Buryatia (Badmaev and Bazarov, 2018). The maximal seasonal depth of thaw varies from 30 to 300 cm in ultra-continental Siberia following the heat and moisture regime, which depends on topography, soil composition, aspect, and vegetation cover, and is thicker than the 18–220 cm layer found in the Arctic ecosystems (Karelin and Zamolodchikov, 2008).

Summers in the inner regions of permafrost zone of Eurasia are extremely hot and arid with 80–150 mm of precipitation and much higher evaporation. This type of climate is similar to zonal semi-deserts and dry steppe. Winters are extremely cold with mean temperatures from −9 to −19 °C and snow cover reaching 30–40 cm.

A question remains if these conditions more extreme if compared to arctic ecosystems. We conducted a discriminant analysis of environmental features and conditions of the studied cryogenic ecosystems. Arctic ecosystems differed substantially from ultra-continental ecosystems (100% of classified cases, $n = 18$ (sites in Table 1)). The most significant functional features of ultra-continental areas compared to the Arctic, were (in order of decreasing significance): (i) lower soil moisture, (ii) more annual above-zero temperature days (Fig. 9), (iii) deeper thaw, and (iv) lower annual precipitation. Permafrost thickness, average soil, and mean annual air temperatures were insignificant discriminant factors.

However, the principal component analysis showed that the main external factors affecting soil CO_2 emissions were the annual sum of positive temperatures and maximal associated depth of thaw, as well as the soil moisture, annual precipitation, and air temperature (Fig. 10). Two principal components explain 85.7% of cumulative variance. In the rotated factors, the sum of positive degree days and thaw depth all have high positive loadings on the first component (explaining 52.2% of total variance), whereas annual precipitation, annual air temperature, and moisture index are highest on the second component. Hence, the first component grouped the factors of total heat income with CO_2 emission, whereas the second component related to moisture regime, linked to the main hydrothermal indexes.

Overall, the ultra-continental ecosystems (UC) compared to arctic (AR) are functioning in dryer and warmer conditions. Positive influence of the last factor blocks the negative effect of dryness resulting in considerably greater CO_2 emission from soil (0.201 ± 0.02 (UC) > 0.076 ± 0.01 g C m^{-2} h^{-1} (AR), median test, $P = 0.009$).

Apart from macro-ecological external factors controlling the general conditions of soil CO_2 fluxes, we separately analysed the internal ecosystem fluxes micro-controls. Evaluation of the most significant CO_2 emission micro-factors in ultra-continental ecosystems was conducted using DistLM. This method allows evaluation of individual numerical contributions of factors to total variance, and it could be applied to overcome limitations of common regression analysis, such as normal distribution of errors for all variables. Additionally, instead of n measurements, this analysis considers $n(n–2)/2$ differences between measurement pairs, which increases the robustness of the statistics when dealing with small datasets and numerous predictors.

To exclude the role of human impacts, only the cryogenic ecosystems with minimal disturbance were included in the analysis (Table 6). The model describes 83% of variance, which is a good correspondence. Among the twelve analysed independent variables only three were significant for the whole dataset: *above-ground phytomass storage* (explains 65.4% of total variance), *presence of tree canopy* (11.1%), and *the degree of soil fissuring* (5.1%). The slope factor was

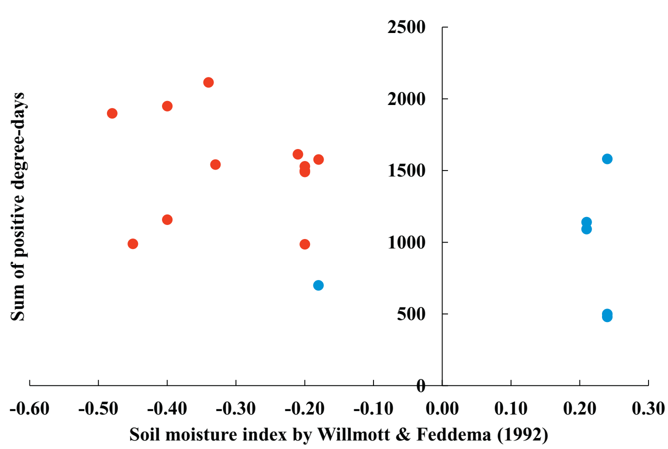

Fig. 9. Main discriminant environmental factors of the studied Arctic and ultra-continental ecosystems (Table 1, $n = 18$): normalised Moisture Index (−1: +1) by Willmott and Feddema (1992), and sum of positive degree days. Negative values of Moisture Index correspond to the arid conditions. Blue markers – arctic ecosystems in study, red – ultra-continental trans-Siberian transect.

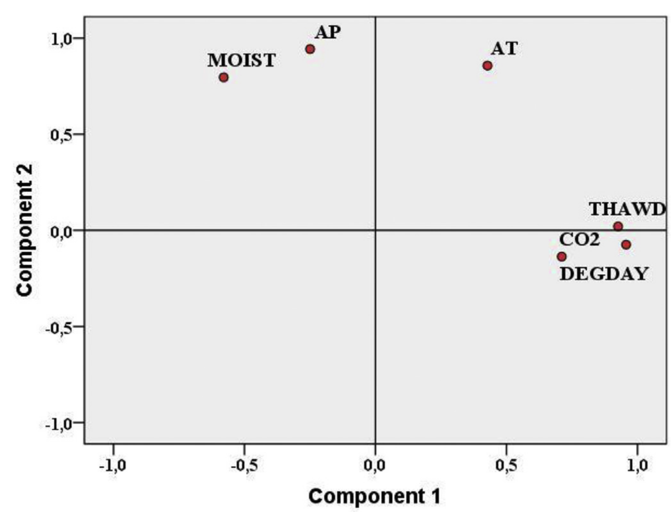

Fig. 10. Component plot in rotated space as output of principal components analysis (Varimax rotation method with Kaiser normalization) of macro-variables and CO_2 soil emission of the studied cryogenic ecosystems (Table 1, $n = 18$). AT – mean annual air temperature, AP – annual precipitation, MOIST – soil Moisture index, THAWD – maximal seasonal depth of thaw, DEGDAY – sum of positive degree-days, CO2 - emission of carbon dioxide from soil.

close to the significance level (1.5%). When ultra-continental ecosystems were excluded from the analysis, phytomass remained the most significant variable; however, *active layer thickness* and *absolute elevation* also started playing a secondary role.

The contribution of the phytomass storage was dominant. The occurrence of trees should be a factor as the tree canopy highly supports permafrost conservation, essentially increasing the input of carbon to soil and directly affecting soil CO_2 emission through mycorrhizal and root respiration and forest fires. When ultra-continental soils were included in the analysis, the new positive emission factor was introduced (fissuring of soil, density of cracks). This factor rarely acts in arctic soils due to excess moisture content. The pronounced network of desiccation cracks in Siberian ultra-continental soils provides aeration to deeper soil layers increasing respiration and supports vertical gas transportation (correlation between CO_2 emission and fissuring of soil: $r_s = +0.80$, $P < 0.01$). The lack of moisture in these ecosystems both reduces soil respiration in the upper horizons, while increasing soil fracturing, which contributes to emissions from the lower soil layers. Therefore, due to the combination of these factors, the surface CO_2 flux increases. Steeper slopes promote additional drainage and leaching of biogenic chemical species from soil, which supports CO_2 transport to the atmosphere, but decreases its production in soil, leading to emission declines. The action of mountain topography was mediated by slope and temperature (correlation between CO_2 emission and absolute elevation: $r_s = +0.62$, $P < 0.01$).

The Spearmen correlation matrix (data not shown) demonstrated that CO_2 emission is also correlated positively with other independent variables, including: absolute elevation, depth of thaw (+0.61), carbon storage in soil (+0.55), and soil temperature at 10 cm (+0.49, $P < 0.01$), and is negatively correlated with soil moisture, (−0.39, $P = 0.014$) and moss-lichen layer thickness (−0.34, $P = 0.035$). These variables were excluded from the model during regression analysis by the program algorithm due to inter-correlations. Those can either correspond to a false relationship (for example, positive correlation of absolute elevation and emission), or real positive/negative feedbacks. Furthermore, inter-correlation between variables may lead to unstable regression estimates, omitting one of them from the model only minimally affects prediction. Pronounced inter-correlation between components and factors is a common feature of all cryogenic ecosystems (Karelin and Zamolodchikov, 2008).

In some cases, it could be difficult to understand the dependent variables, for example; phytomass storage was significantly correlated to fissuring of soil ($r_s = +0.58$, $P < 0.01$), elevation (+0.53, $P < 0.01$), carbon storage (+0.43, $P < 0.01$), active layer (+0.37, $P < 0.05$), and soil moisture (−0.38, $P < 0.05$). Soil fissuring was also significantly linked to tree occurrence, elevation, carbon storage in soil, thickness of mosses and lichens cover, active layer thickness, and soil temperature and moisture. Hence, the variables of phytomass, tree occurrence, and crack appearance accounted for the other linked factors not included into the model. Above-ground phytomass and tree occurrence are the key factors because they not only depend on climate, soil, slope, and other factors, but also actively transform the environment affecting soil depth, SOC content, fissuring, micro-topography, and soil moisture and temperature, which mediate microbial activity, root respiration, and gas transport.

The cumulative effect of all significant factors increased soil emissions in the ultra-continental permafrost zone compared to the Arctic. The ratio between CO_2 emission in forested and open biotopes in ultra-continental and arctic ecosystems is shown in Fig. 11. Both forested and open ultra-continental landscapes emitted more soil CO_2 per unit area than Arctic ecosystems. We conclude that this is due to greater above-ground phytomass storage, tree occurrence, deeper thaw, larger carbon storage, and expressed soil fissuring, as well. All these micro-ecological (internal) factors are in turn driven by external climatic micro-controls discussed above.

3.2.2. Soil GHGs emission in alas depressions

There are around 16,000 thermokarst depressions, also known as "alas", located in the Central Yakutia lowland within the boreal forest region. These formations are specific to this areaand were formed due to thawing of ice wedges. The alases cover 17% of the total land area of Central Yakutia (Desyatkin et al., 2007), with local estimates between 20% (Tungulu plain) and 75% on seaside wetlands (Yana-Indigirka and Indigirka-Kolyma plains) (Roman V. Desyatkin, personal communication, July 29, 2018). Alases have been used by Yakuts (Sakha tribes) as hay and grazing lands for a many years, which has caused their recent degradation. Due to their formation under thermokarst lakes, they possess the highest soil carbon storages compared to other permafrost ecosystems (28–74 kg C m^{-2} in central parts of alases according to our estimates and Matsuura et al., 1994) and high primary production (Danilova et al., 2013). Warmer and wetter microclimates and manure subsidies due to grazing provide additional contributions to primary production. Soils of alases have no analogues in terms of conditions, development, dynamics, and metamorphism, causing a very complicated soil structure. They have different grades of salinization and specific classification (Desyatkin, 1984). Compared to other ultra-continental zone cryogenic ecosystems, many studies have been conducted on biogenic GHG fluxes in alases (Desyatkin et al., 2007, 2009).

A basic profile of a mature alas depression is represented by a central lake surrounded by wetlands and an aerially dominant meadow zone. A thawed layer ("talik") forms down to several meters below the lake bottom in the centre of the alas and its outer ring is formed by a steppe-like arid plant community (Bosikov, 1991). In studies, the depth of thaw rapidly decreased from 3 to 1.17 m (August 2017) from the centre to periphery of the alas, where a larch-birch (*Larix gmelinii, Betula platyphylla*) forest grew. The alas cross-section (Fig. 12) shows a decreasing gradient of soil moisture. From the waterlogged centre to elevated periphery of the alas, volumetric moisture in 0–7 cm of soil decreased from 56.6 to 17.6% and soil temperature in the topmost 1 cm rose from 9.4 to 24.9 °C. The optimum hydrothermal regime for aerobic respiration of roots, fungi, and bacteria in the soil is achieved in the intermediate meadow belt, the total respiration of the soil community increases and then decreases, which is clearly reflected in the observed rate of CO_2 emission (Fig. 12). This regime also promotes higher primary production in the meadow zone.

Measurements made by Desyatkin A.R. and colleagues on the alas nearby (N62°09′08″, E130°31′42″) in April–September 2006–2009 showed that lake water surface emitted negligible amounts of CO_2 ($+0.009 \pm 0.0004$ g C m^{-2} h^{-1}, $n = 30$) and nitrous oxide ($+0.0012 \pm 0.0003$ mg N_2O m^{-2} h^{-1}, $n = 6$). The area-weighted alas CO_2 flux (including lake) comprises $+0.128 \pm 0.008$ g C m^{-2} h^{-1}, which is significantly less than in other ultra-continental biotopes ($+0.201 \pm 0.020$, $P < 0.01$). Thus, alases do not negatively influence regional CO_2 fluxes.

However, methane ($+1.61 \pm 0.90$ mg CH_4 m^{-2} h^{-1}, $n = 9$) and nitrous oxide ($+0.29 \pm 0.20$ mg N_2O m^{-2} h^{-1}, $n = 9$) fluxes in meadows and wetlands of alas depressions were the highest among all studied arctic and ultra-continental ecosystems. Our estimates were comparable to long-term monitoring of methane ($+6.7 \pm 2.5$, $n = 30$) and nitrous oxide (-0.0023 ± 0.0007, $n = 30$) in alas wetland soil (Desyatkin et al., 2009). Such methane fluxes were caused by one of the highest storages of SOC in the active cryolithozone layer, and higher moisture content and soil temperature in the vegetation period.

In all other studied ultra-continental ecosystems, methane and nitrous oxide fluxes were very small and insignificantly differed from zero (-0.005 ± 0.125 mg CH_4 m^{-2} h^{-1} ($n = 24$); -0.003 ± 0.004 mg N_2O m^{-2} h^{-1}, $n = 24$), which is mostly due to high aridity. Note, that alas lakes were a much stronger source of methane reaching 0.876–10.7 mg CH_4 m^{-2} h^{-1} (recalculated from data by Desyatkin et al. (2009)), which does not differ from open waters in other boreal ecosystems (Sabrekov et al., 2017). However, against the generally very low

Table 6
DistLM of relative and absolute contribution of CO_2 emission micro-controls from soils in cryogenic ecosystems (August 2017, sites included correspond to the numbers 1–18 in Table 1).[a]

Independent variables	Resulting Akaike Information Criterion	Pseudo-F criterion	P (significance level)	Proportion of variance explained by each variable	Cumulative proportion of variance explained by included variables	Degrees of freedom
PHYTO	−191.03	67.989	0.001	0.65381	0.65381	36
BIOTOPE	−203.64	16.398	0.001	0.11045	0.76426	35
CRACK	−210.8	9.277	0.005	5.0534E-2	0.81479	34
SLOPE	−211.89	2.7943	0.088	1.4458E-2	0.82925	33

[a] Dependent variable – CO_2 efflux from soil. Independent variables included into the model: PHYTO – above-ground phytomass storage (t ha^{-1}), BIOTOPE – presence of forest canopy, CRACK – density of cryogenic and desiccation crack network at the soil surface (categories from 0 to 5, see Section 2.5), SLOPE – slope of surface (degrees). Significant variables are in bold. Independent variables excluded from the analysis as insignificant: total SOC storage in active permafrost layer (kg m^{-2}); total nitrogen storage in active permafrost layer (kg m^{-2}); pH (water) in the topmost 10 cm of soil; volumetric moisture in the topmost 0–7 cm; temperature at the depth of 10 cm, elevation (a.s.l); meso-relief (nominal: automorphic, mesomorphic, or hydromorphic); micro-relief (nominal: micro-depression or micro-elevation); maximal depth of thaw (cm); thickness of moss-lichen layer (cm).

methane fluxes in the cryolithozone, especially on automorphic relief forms (Desyatkin et al., 2009), this contribution may be significant.

Thus, despite the aridity, higher heat inflow contributes to increased CO_2 emissions from soil during the vegetation period in the ultra-continental permafrost regions as compared to the Arctic. However, the aridity essentially decreases the fluxes of methane and nitrous oxide. The exception is in permafrost thermokarst depressions (alases), which with their wide representation in the relief of Central Yakutia, can significantly increase methane emissions in regional landscapes.

3.2.3. Features of the Birch effect in ultra-continental ecosystems

Studies of a transient increase in soil carbon dioxide and nitrogen oxides efflux after rewetting of previously dry soils, widely known as the BE (Birch, 1958), continue. Controls and mechanisms of sharp multifold increases in gas emissions after moistening of a dry soil and contribution of these fluxes to GHG balances have been examined (Unger et al., 2010, 2012; Lopes de Gerenyu et al., 2018). However, it is rarely used to compare ecosystem functionality (Karelin et al., 2017a). It was shown by Unger et al. (2010) that the initial (less than 1 h) strong short-term CO_2 emission event from soil is mainly caused by two processes linked to microbial activity in dry soil after rewetting: reassimilation of hypo-osmotic microbial compounds and assimilation of dead microbial cells. Both processes are directly linked to a number of live microorganisms. Thus, our technique with the 20 min delay after rewetting reflected a number and activity of soil microorganisms before their multiplication. The natural initiator of BE is precipitation, which was simulated in our case by addition of a standard amount of distilled water per unit area (Section 2.3). Apart from the soil moisture factor, BE, as well as heterotrophic respiration of soil microorganisms

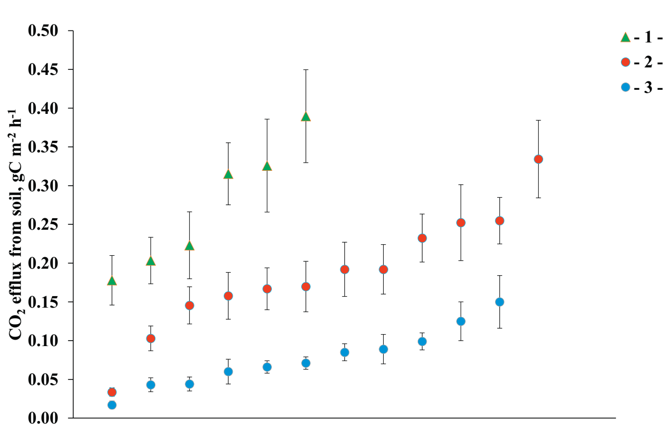

Fig. 11. The CO_2 fluxes from soil in different ecosystems of the Siberian ultra-continental zone (UC) vs. arctic ecosystems. 1 – larch–birch forests (UC), 2 – low stature tundra-like, steppe-like or meadow biotopes (UC), 3 – tundra ecosystems in the Arctic. All data are sorted in ascending order. Means and standard errors are given ($n = 10 \div 45$).

and non-mycorrhizal fungi in general, are functions of the amount of labile soil carbon (Scott-Denton et al., 2006) and available nitrogen (Birch, 1958). Generally, the higher the moisture stress in soil and labile carbon and nitrogen compounds, the higher is the BE. Therefore, from an environmental point of view, BE can be considered as an indicator of water and nutrition stress in soil microbial communities, that can be easily assessed in a field.

In fact, BE is a feature of all insufficiently moistened soils (Karelin et al., 2017a). Lengthy soil droughts are rare in tundra even in the middle of summer (Karelin and Zamolodchikov, 2008). Thus, the addition of water to soils did not produce any significant increase in respiration. The CO_2 emission values in Vorkuta tundra after the rewetting experiments were never significantly different from initial rates: 1.2 ± 0.3 (a ratio between emission rate after water addition and initial rate; $n =$ 54, 2010–2018). Water is found in tundra soils at nearly all times because of the proximity of the permafrost table and low evaporation. However, there are limitations for roots set by low temperature of capillary water from the thawing permafrost on automorphic uplands in summer.

By contrast, BE was significantly higher (2.53 ± 0.78 ($P < 0.05$, $n =$ 85)) in ultra-continental ecosystems due to local soil aridity. The average moisture contents in the upper soil layer significantly differed (18.3 ± 2.2% (ultra-continental, $n = 210$) < 43.2 ± 5.8% (arctic, $n =$ 170), $P < 0.05$), even though the range of variability was similar. The fact that in ultra-continental soils the depth of the active permafrost layer is greater due to the higher heat input creates additional problems with the water inflow to the active layer of soil from the seasonally thawing permafrost.

It is of interest to compare the estimates of artificial BE obtained using same technique for ultra-continental soils and the main zonal types of soils on the European territory of Russia (Karelin et al., 2017a) depending on the moisture content of the topsoil layer. European soils range northward from kastanozems with calcisol–solonetz complexes in semi-arid steppe environments (N47.5°, E46°) to the forest-steppe chernozems (N51.5°, E36°), luvic phaeozems in broadleaved forests (N53°, E35°), albeluvisols in mixed forests (N55°, E34°), and podzols in the southern taiga (N58°, E33°), which demonstrated strong linear correlation of BE to soil moisture (Fig. 13). While various types of ultra-continental soils have moisture content in the range of 15–25%, they did not show any relationship. Cryoarid soils found on a steep southeastern slope of 35° in Yakutya (Table 1, site 15) with volumetric moisture content of 5% were an exception with an increase in respiration of 15.4 ± 3.1, similar to the kastanozems of the European steppe zone (Fig. 13).

Such a weak response of the soils in the medium moisture content range compared to European soils could have two reasons: lack of labile carbon and nitrogen caused by the small pool of microbial cells, and the influence of other unaccounted physicochemical features of the soils limiting the rate of microbial nutrient assimilation. Such responses could be considered long-term adaptations of the ultra-continental permafrost soil microbial population to extreme aridity.

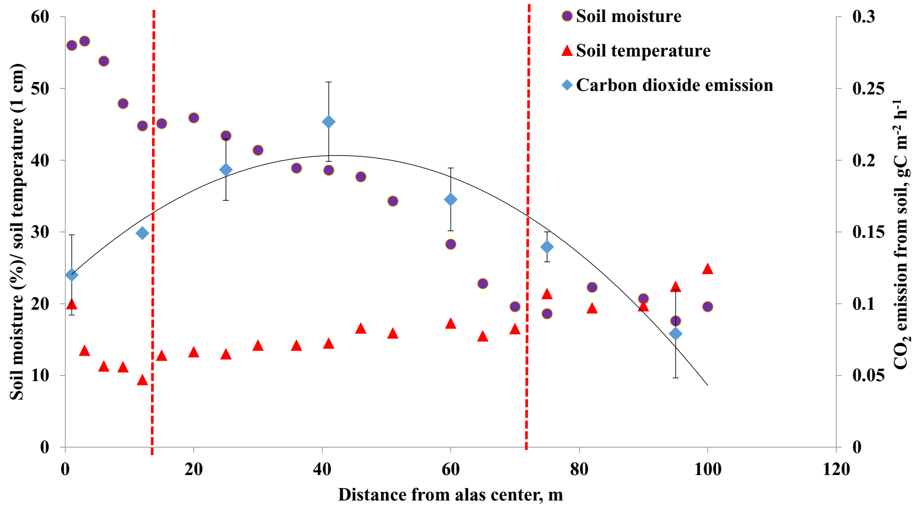

Fig. 12. The cross-section of an alas depression with CO_2 soil emissions (Yakutia, August 2017, site AL1, Table 1) vs. volumetric soil moisture in topmost 0–7 cm and soil temperature at 1 cm depth. Means and standard errors and parabolic regression line for CO_2 emission are given. The vertical dashed lines mark the limits of boggy-meadow, meadow-like, and steppe-like alas zones, from left to right.

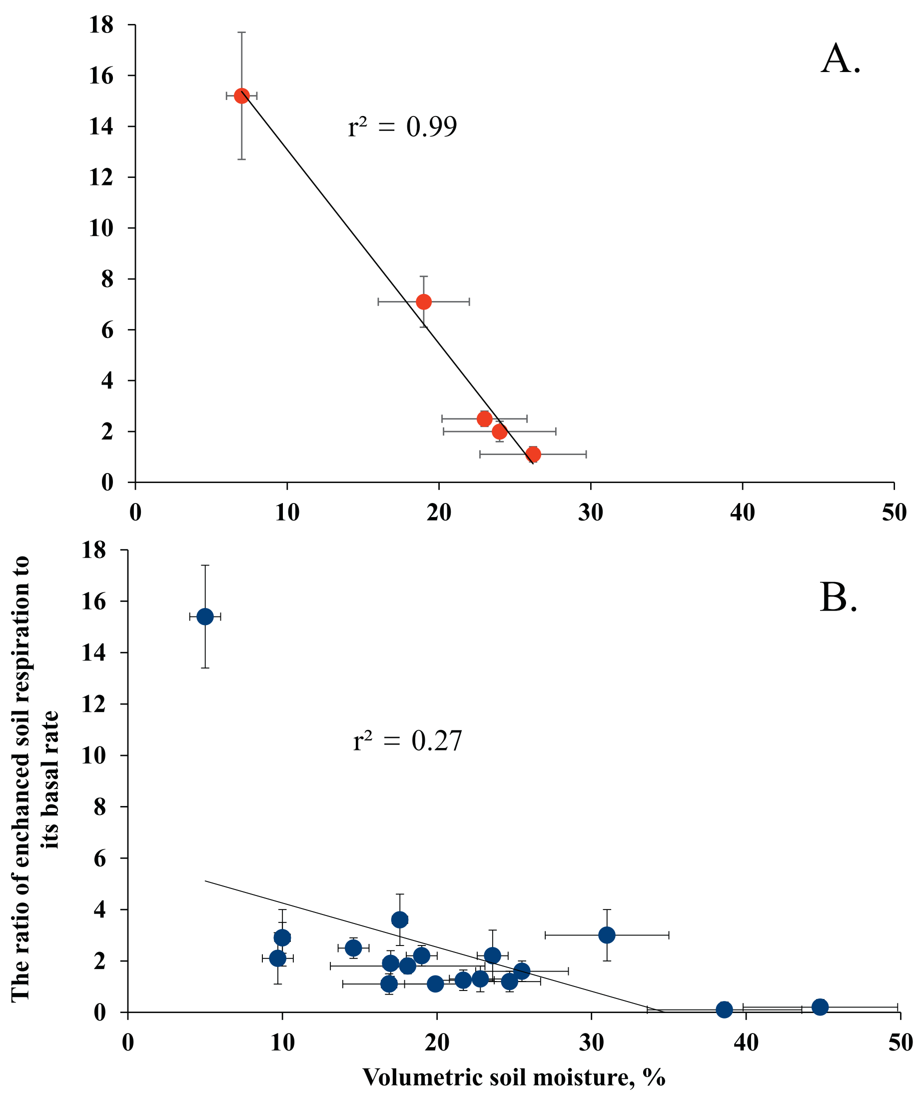

Fig. 13. The rise in initial CO_2 soil emission due to artificial Birch effect measured in the field vs. volumetric soil moisture in 0–7 cm of topsoil: A. in different zonal ecosystems of European Russia in August 2012–2014 (a – podzols in southern taiga ($n = 30$), b – albeluvisols in mixed forests ($n = 20$), c – luvic phaeozems in broad-leaved forests ($n = 30$), d – forest-steppe chernozems ($n = 30$), and f – dry steppe kastanozems with calcisol–solonetz soil complexes ($n = 30$); modified from Karelin et al. (2017a); B. in ultra-continental soils in Central and Northeast Siberia (present study; points represent sites in the study, for each point $n = 5$). Means and standard errors are given.

With the exception of sparsely distributed cryoarid soils, the observed regularity evidenced that these soils cannot be considered as additional pulse sources of CO_2 for the atmosphere after precipitation events, which is typical for soils under seasonally dry climates in response to rewetting after drought periods (Lopes de Gerenyu et al., 2018; Unger et al., 2012).

4. Conclusion

Regional- and local-scale studies showed that local land use always significantly alters emissions of CO_2, CH_4, and N_2O from permafrost- and cold-affected soils of Eurasia. The sites with land use in most cases converted into net CO_2 sources and exhibited decreased methane emissions; however, certain types of land use (flooded areas along elevated subgrades and embankments) increased CO_2 sequestration and methane emission. Other types of land use (coalmine shafts and dirt roads under operation) could increase background soil CO_2 emission by one order of magnitude. The most significant effects of land use were imposed by destruction of the vegetation cover and deeper thawing of permafrost, the key controls of CO_2 fluxes in natural cryogenic ecosystems. Consequences of fires for the carbon balance lasted for tens of years. Local drainage effects were more significant for methane emission. In general, land use factors reinforced soil emissions and net sources of CO_2 and N_2O and weakened methane sources.

Siberian ultra-continental permafrost landscapes were similarly controlled by the factors of GHG balance in the Arctic. However, higher aridity and heat supply compared to the Arctic provided some specific features. High aridity, even under extended heat supply, caused significantly lower emission of methane and nitrous oxide. However, these climatic features support higher CO_2 emission rates from soil due to larger phytomass storage, presence of a tree canopy, thicker active permafrost layer, and more expressed soil fissuring. In addition, the BE is much less expressed in ultra-continental permafrost soils than in permafrost-free European soils. We hypothesise that this is mostly due to the smaller microbial pool in these soils or some physicochemical limitations of assimilation by microbiota of hypo-osmotic microbial compounds and dead microbial cells in rewetted soil. The last feature nullifies the potential pulse contribution of BE to annual fluxes of SR in ultra-continental permafrost zone.

It is clear that areal estimates of contribution of local human impacts on soil and net GHG fluxes had significant seasonal variations. Moreover, the anthropogenic impact on the release of CO_2 from soils is comparable to the impact of climate change on it at similar times. Settlements and industrial areas in the tundra function as a year-round net CO_2 sources mostly due to the lack of vegetation cover. Therefore, they could compensate the natural C-balance on significantly larger areas of surrounding tundra.

Recently, the tundra biome acted as a C-sink during the growing season, and an atmospheric source on an annual basis (Belshe et al., 2013). Future climate warming was forecasted to transform it into a source, primarily with additional CO_2 from thawing permafrost and extended microbial CO_2 emission from soil (Heimann and Reichstein, 2008). Moreover, local human land use impacts in this relatively unexplored domain will undoubtedly support conversion of tundra to a GHG source. The main factors driving this are destruction of vegetation and soil cover, causing further permafrost thawing and growth of CO_2 and N_2O emissions. The anticipated decrease in CH_4 emissions from local human impact due to draining might be compensated by additional emissions from thawing permafrost (Kraev et al., 2013).

Tundra and permafrost are large storage reservoirs of organic carbon on our planet. Fluxes of biogenic GHGs in tundra in general are an order of magnitude smaller than in forests. However, they are harder to regulate and thus, are governed by climate fluctuations. Local land use regulation in the tundra biome and permafrost zone could serve such a control through prevention of fires, remediation of lands, and conservation.

Declaration of competing interest

Authors declare no conflicts of interest.

Acknowledgements

We thank editors and anonymous reviewers for their useful comments that helped to improve the manuscript.

Funding

This work was funded by the Russian Foundation for Basic Research (18-05-60279-Arctica). Field studies in Svalbard, Naryan-Mar, Bovanenkovo, and the vicinities of Vorkuta were carried out within the framework of the State assignment 0148-2019-0006 (Institute of Geography, Russian Academy of Sciences (RAS)), laboratory work at the Institute of Forest Science, RAS was supported by the Russian Science Foundation (19-74-20185). Field studies in Buryatia were supported by the research projects 0337-2017-0002 and 0337-2017-0006 of the Institute of General and Experimental Biology of the Siberian Branch, RAS.

References

Anderson, J.P.E., Domsch, K.H., 1978. A physiological method for the quantitative measurement of microbial biomass in soils. Soil Biol. Biochem. https://doi.org/10.1016/0038-0717(78)90099-8.

Badmaev, N., Bazarov, A., 2018. Monitoring network for atmospheric and soil parameters measurements in permafrost area of Buryatia. Russ. Fed. Geosci. https://doi.org/10.3390/geosciences9010006.

Badmaev, N.B., Konyushkov, D.E., Kulikov, A.I., Lesovaya, S.N., Mergelov, N.S., Titova, A.A., Turova, I.V., Goryachkin, S.V., 2009. Pochvy i temperaturnye rezhimy tsentral'noi Buryatii i vostochnogo Pribaikal'ya (Soils and temperature regimes of the Central Buryatia and the West Transbaikal mountains). Guidebook for Field Excursions of the 5th International Conference on Cryopedology. Izd-vo IG RAN, Moscow.

Bazilevich, N.I., 1993. Biologicheskaya Produktivnost' Ekosistem Severnoi Evrazii (Biological Productivity of Ecosystems in Northern Eurasia). Nauka, Moscow.

Belshe, E.F., Schuur, E.A.G., Bolker, B.M., 2013. Tundra ecosystems observed to be CO_2 sources due to differential amplification of the carbon cycle. Ecol. Lett. https://doi.org/10.1111/ele.12164.

Berestovskaya, Y.Y., Rusanov, I.I., Vasil'eva, L.V., Pimenov, N.V., 2005. The processes of methane production and oxidation in the soils of the Russian Arctic tundra. Microbiology https://doi.org/10.1007/s11021-005-0055-2.

Birch, H.F., 1958. The effect of soil drying on humus decomposition and nitrogen availability. Plant Soil https://doi.org/10.1007/BF01343734.

Bosikov, N.P., 1991. Evolyutsiya Alasov Tsentral'noi Yakutii (Evolution of Alases in Central Yakutia). Izd-vo IMZ, Yakutsk.

Chen, Q., Zhu, R., Wang, Q., Xu, H., 2014. Methane and nitrous oxide fluxes from four tundra ecotopes in Ny-Ålesund of the High Arctic. J. Environ. Sci. (China) https://doi.org/10.1016/j.jes.2014.05.005.

Chestnykh, O.V., Zamolodchikov, D.G., 2018. Pochvennye kharakteristiki Severnoi Evrazii (Features of soils in northern Eurasia) Rospatent, RU 2018621164. [Dataset].

Curry, C.L., 2007. Modeling the soil consumption at atmospheric methane at the global scale. Glob. Biogeochem. Cycles https://doi.org/10.1029/2006GB002818.

Danilova, A.A., Danilov, P.P., Savvinov, G.N., Gavrilyeva, L.D., Petrov, A.A., Alekseev, G.A., 2013. Changes in properties of alas soils in Central Yakutia caused by pasture degradation. Arid. Ecosyst. 3, 205–211. https://doi.org/10.1134/S2079096113040057.

Desyatkin, R.V., 1984. Pochvy Alasov Leno-Amginskogo Mezhdurechya (Soils of Alases of Lena and Amga Interfluve). Izd-vo YaF SO AN SSSR, Yakutsk.

Desyatkin, A.R., Takakai, F., Fedorov, P.P., Desyatkin, R.V., 2007. Effect of human activity on carbon balance in meadows in a thermokarst depression in Siberia. Eurasian J. For. Res. 10, 89–96.

Desyatkin, A.R., Takakai, F., Fedorov, P.P., Nikolaeva, M.C., Desyatkin, R.V., Hatano, R., 2009. CH_4 emission from different stages of thermokarst formation in central Yakutia. East Siberia Soil Sci. Plant Nutr. https://doi.org/10.1111/j.1747-0765.2009.00389.x.

French, H.M., 1996. The Periglacial Environment. 2nd ed. Longman, Harlow.

Heimann, M., Reichstein, M., 2008. Terrestrial ecosystem carbon dynamics and climate feedbacks. Nature https://doi.org/10.1038/nature06591.

Karelin, D.V., Zamolodchikov, D.G., 2008. Uglerodnyi Obmen V Kriogennykh Ekosistemakh (Carbon Exchange in Cryogenic Ecosystems). Nauka, Moscow.

Karelin, D.V., Zamolodchikov, D.G., Zukert, N.V., Chestnykh, O.V., Pochikalov, A.V., Kraev, G.N., 2013. Interannual changes in PAR and soil moisture during the warm season may be more important for directing of annual carbon balance in tundra than temperature fluctuations. Zh. Obshch. Biol. 74, 3–22.

Karelin, D.V., Goriachkin, S.V., Zamolodchikov, D.G., Dolgikh, A.V., Zazovskaya, E.P., Shishkov, V.A., Pochikalov, A.V., Sirin, A.A., Suvorov, G.G., Kraev, G.N., 2016. Vliyanie mestnykh antropogennykh faktorov na pochvennuyu emissiyu biogennykh parnikovykh gazov v kriogennykh ekosistemakh (The influence of local anthropogenic factors on soil emission of biogenic greenhouse gases in cryogenic ecosystems). Zh. Obshch. Biol. 77, 167–181.

Karelin, D.V., Dolgikh, A.V., Kudikov, A.V., Lunin, V.N., Goryachkin, S.V., Lyuri, D.I., Lopes de Gerenyu, V.O., 2017a. Changes in carbon pool and CO_2 emission in the course of post-agrogenic succession on gray soils (Luvic phaeozems) in European Russia. Eurasian Soil Sci. https://doi.org/10.1134/s1064229317050076.

Karelin, D.V., Goryachkin, S.V., Zamolodchikov, D.G., Dolgikh, A.V., Zazovskaya, E.P., Shishkov, V.A., Kraev, G.N., 2017b. Human footprints on greenhouse gas fluxes in cryogenic ecosystems. Dokl. Earth Sci. 477, 1467–1469. https://doi.org/10.1134/S1028334X17120133.

Karelin, D.V., Zamolodchikov, D.G., Kaganov, V.V., Pochikalov, A.V., Gitarskii, M.L., 2017c. Microbial and root components of respiration of sod-podzolic soils in boreal forest. Contemp. Probl. Ecol. 10, 717–727. https://doi.org/10.1134/S199542551707006X.

Kovda, I., Goryachkin, S., Lebedeva, M., Chizhikova, N., Kulikov, A., Badmaev, N., 2017. Vertic soils and vertisols in cryogenic environments of southern Siberia, Russia. Geoderma https://doi.org/10.1016/j.geoderma.2016.11.008.

Kraev, G.N., Schultze, E.-D., Rivkina, E.M., 2013. Cryogenesis as a factor of methane distribution in layers of permafrost. Dokl. Earth Sci. https://doi.org/10.1134/s1028334x13080291.

Kuzyakov, Y., 2006. Sources of CO_2 efflux from soil and review of partitioning methods. Soil Biol. Biochem. https://doi.org/10.1016/j.soilbio.2005.08.020.

Lopes de Gerenyu, V.O., Kurganova, I.N., Khoroshaev, D.A., 2018. The effect of contrasting moistening regimes on CO_2 emission from the gray forest soil under a grass vegetation and bare fallow. Eurasian Soil Sci. https://doi.org/10.1134/s1064229318100034.

Marushchak, M.E., Pitkämäki, A., Koponen, H., Biasi, C., Seppälä, M., Martikainen, P.J., 2011. Hot spots for nitrous oxide emissions found in different types of permafrost peatlands. Glob. Chang. Biol. https://doi.org/10.1111/j.1365-2486.2011.02442.x.

Marushchak, M.E., Friborg, T., Biasi, C., Herbst, M., Johansson, T., Kiepe, I., Liimatainen, M., Lind, S.E., Martikainen, P.J., Virtanen, T., Soegaard, H., Shurpali, N.J., 2016. Methane dynamics in the subarctic tundra: combining stable isotope analyses, plot- and ecosystem-scale flux measurements. Biogeosciences https://doi.org/10.5194/bg-13-597-2016.

Matsuura, Y., Ohta, S., Sanada, M., Desyatkin, R.V., 1994. Carbon and nitrogen storage in soil developed on two different toposequences of the Lena River terrain. In: Inoue, G. (Ed.), Proceedings of the Second Symposium on the Joint Siberian Permafrost Studies between Japan and Russia in 1993 (Tsukuba, 13–14 January 1993). Isebu, Tsukuba, pp. 177–182.

Oertel, C., Matschullat, J., Zurba, K., Zimmermann, F., Erasmi, S., 2016. Greenhouse gas emissions from soils – a review. Chem. Erde-Geochem. https://doi.org/10.1016/j.chemer.2016.04.002.

Pachauri, R.K., Allen, M.R., Barros, V.R., Broome, J., Cramer, W., Christ, R., van Ypersele, J.-P. (Eds.), 2015. Climate Change 2014: Synthesis Report. Contribution of Working Groups I, II and III to the Fifth Assessment Report of the Intergovernmental Panel on Climate Change. IPCC, Geneva. https://doi.org/10.1017/CBO9781107415324.004.

Pandey, D., Agrawal, M., Pandey, J.S., 2011. Carbon footprint: current methods of estimation. Environ. Monit. Assess. https://doi.org/10.1007/s10661-010-1678-y.

Petrescu, A.M.R., Lohila, A., Tuovinen, J.-P., Baldocchi, D.D., Desai, A.R., Roulet, N.T., Vesala, T., Dolman, A.J., Oechel, W.C., Marcolla, B., Friborg, T., Rinne, J., Matthes, J.H., Merbold, L., Meijide, A., Kiely, G., Sottocornola, M., Sachs, T., Zona, D., Varlagin, A., Lai, D.Y.F., Veenendaal, E., Parmentier, F.-J.W., Skiba, U., Lund, M., Hensen, A., van Huissteden, J., Flanagan, L.B., Shurpali, N.J., Grünwald, T., Humphreys, E.R., Jackowicz-Korczyński, M., Aurela, M.A., Laurila, T., Grüning, C., Corradi, C.A.R., Schrier-Uijl, A.P., Christensen, T.R., Tamstorf, M.P., Mastepanov, M., Martikainen, P.J., Verma, S.B., Bernhofer, C., Cescatti, A., 2015. The uncertain climate footprint of wetlands under human pressure. Proc. Natl. Acad. Sci. https://doi.org/10.1073/pnas.1416267112.

Sabrekov, A.F., Runkle, B.R.K., Glagolev, M.V., Terentieva, I.E., Stepanenko, V.M., Kotsyurbenko, O.R., Maksyutov, S.S., Pokrovsky, O.S., 2017. Variability in methane emissions from West Siberia's shallow boreal lakes on a regional scale and its environmental controls. Biogeosciences https://doi.org/10.5194/bg-14-3715-2017.

Savvinov, D.D., 1976. Gidrotermicheskii Rezhim Pochv V Zone Mnogoletnei Merzloty (Hydrothermic Regime of Soils in Permafrost Zone). Nauka, Novosibirsk.

Schulze, E.D., Luyssaert, S., Ciais, P., Freibauer, A., Janssens, I.A., Soussana, J.F., Smith, P., Grace, J., Levin, I., Thiruchittampalam, B., Heimann, M., Dolman, A.J., Valentini, R., Bousquet, P., Peylin, P., Peters, W., Rödenbeck, C., Etiope, G., Vuichard, N., Wattenbach, M., Nabuurs, G.J., Poussi, Z., Nieschulze, J., Gash, J.H., 2009. Importance of methane and nitrous oxide for Europe's terrestrial greenhouse-gas balance. Nat. Geosci. https://doi.org/10.1038/ngeo686.

Scott-Denton, L.E., Rosenstiel, T.N., Monson, R.K., 2006. Differential controls by climate and substrate over the heterotrophic and rhizospheric components of soil respiration. Glob. Chang. Biol. https://doi.org/10.1111/j.1365-2486.2005.01064.x.

Smagin, A.V., Dolgikh, A.V., Karelin, D.V., 2016. Experimental studies and physically substantiated model of carbon dioxide emission from the exposed cultural layer of Velikii Novgorod. Eurasian Soil Sci. https://doi.org/10.1134/s1064229316040116.

Climate change 2007 – the physical science basis. In: Solomon, S., Qin, D., Manning, M., Marquis, M., Averyt, K., Tignor, M.M.B., Miller Jr., H.L., Chen, Z. (Eds.), Working Group I Contribution to the Fourth Assessment Report of the IPCC, Cambridge University Press. Cambridge University Press, New York.

Stark, S., Männistö, M.K., Ganzert, L., Tiirola, M., Häggblom, M.M., 2015. Grazing intensity in subarctic tundra affects the temperature adaptation of soil microbial communities. Soil Biol. Biochem. https://doi.org/10.1016/j.soilbio.2015.02.023.

Tarnocai, C., Canadell, J.G., Schuur, E.A.G., Kuhry, P., Mazhitova, G., Zimov, S., 2009. Soil organic carbon pools in the northern circumpolar permafrost region. Glob. Biogeochem. Cycles https://doi.org/10.1029/2008GB003327.

Unger, S., Máguas, C., Pereira, J.S., David, T.S., Werner, C., 2010. The influence of precipitation pulses on soil respiration – assessing the "Birch effect" by stable carbon isotopes. Soil Biol. Biochem. https://doi.org/10.1016/j.soilbio.2010.06.019.

Unger, S., Máguas, C., Pereira, J.S., David, T.S., Werner, C., 2012. Interpreting post-drought rewetting effects on soil and ecosystem carbon dynamics in a Mediterranean oak savannah. Agric. For. Meteorol. https://doi.org/10.1016/j.agrformet.2011.10.007.

WebWIMP, 2009. The Web-Based, Water-Budget, Interactive, Modeling Program. [WWW Document]. URL. http://climate.geog.udel.edu/~wimp/wimp_map.php (accessed 3.11.19).

Williams, P.J., Smith, M.W., 1989. The Frozen Earth. Fundamentals of Geocryology. Cambridge University Press, Cambridge https://doi.org/10.1017/CBO9780511564437.

Willmott, C., Feddema, J., 1992. A more rational climatic moisture index. Prof. Geogr. https://doi.org/10.1111/j.0033-0124.1992.00084.x.

Zamolodchikov, D.G., Karelin, D.V., 2001. An empirical model of carbon fluxes in Russian tundra. Glob. Chang. Biol. https://doi.org/10.1046/j.1365-2486.2001.00380.x.

Zamolodchikov, D.G., Karelin, D.V., Ivaschenko, A.I., 1997. Carbon balance of tundra landscapes in Central Siberia: observations, computer simulation and GIS-modeling. Zh. Obshch. Biol. 58, 15–34.

Zamolodchikov, D.G., Karelin, D.V., Ivaschenko, A.I., 1998a. Postfire alterations of carbon balance in tundra ecosystems: possible contribution to climate change. In: Lewkowicz, A.G., Allard, M. (Eds.), 7th International Conference on Permafrost (Yellowknife, 23–27 June 1998). Université Laval, Centre d'études nordiques, Quebec, pp. 1207–1212.

Zamolodchikov, D.G., Karelin, D.V., Ivashchenko, A.I., 1998b. Post-fire changes of the carbon cycle in southern tundra. Russ. J. Ecol. 29, 236–240.

Zamolodchikov, D.G., Karelin, D.V., Ivaschenko, A.I., Oechel, W.C., Hastings, S.J., 2003. CO_2 flux measurements in Russian Far East tundra using eddy covariance and closed chamber techniques. Tellus B 55, 879–892.

Zamolodchikov, D.G., Utkin, A.I., Korovin, G.N., 2005. Konversionnye koeffitsienty fitomassa/zapas v svyazi s dendrometricheskimi pokazatelyami i sostavom drevostoev (Conversion coefficients of phytomass vs. reserves related to dendrometric parameters and stand composition). Lesovedenie 73–81.